REVIEW

National Science Open
5: 20250052, 2026
https://doi.org/10.1360/nso/20250052

Materials Science

Special Topic: Intelligent Materials and Devices

Dynamic radiation thermal management: Mechanism, multi-band, multimode, and application

Yanrong Jiao[1,2,#], Zhongshao Li[1,2,#], Aibin Huang[1,2], Xiaowei Ji[1,2], Ping Jin[1], Hongjie Luo[3] & Xun Cao[1,2,*]

[1]*State Key Laboratory of High Performance Ceramics and Superfine Microstructure, Shanghai Institute of Ceramics, Chinese Academy of Sciences, Shanghai 200050, China;*
[2]*College of Materials Science and Opto-Electronic Technology, University of Chinese Academy of Sciences, Beijing 100049, China;*
[3]*Institute for the Conservation of Cultural Heritage, Shanghai University, Shanghai 200444, China*

#Contributed equally to this work.
*Corresponding author (email: cxun@mail.sic.ac.cn)

Received 15 September 2025; Revised 9 December 2025; Accepted 15 December 2025; Published online 28 December 2025

Abstract: Amid the global population surge and escalating energy demands, the energy crisis has become increasingly urgent, highlighting the need for the development of green technologies. Radiative thermal management enhances energy efficiency and reduces consumption by dynamically regulating the exchange of solar radiation (visible-near infrared) and inter-object radiative heat (mid-infrared). Utilising certain dynamically responsive smart materials, visible (VIS), near-infrared (NIR), and mid-infrared (MIR) spectrums can be dynamically modulated under external field influences. This paper reviewed the principles and advantages of visible, near-infrared, and mid-infrared light modulation from the perspectives of reflection, scattering, and absorption. It provides guidance for optimizing band-specific regulation and explores corresponding optical behavior modulation in application scenarios based on opaque and transparent systems. Furthermore, it focuses on multi-band, multi-mode optical behavior control methods for smart windows, analyzes the advantages and challenges of their future applications, and proposes recommendations for future development.

Keywords: optics, dynamic, radiation thermal management, multi-band, multimode

INTRODUCTION

With the rapid growth of the global population, continuous improvement in living standards, and rapid industrial development, energy consumption has surged dramatically. This has brought with it thermal comfort issues arising from complex and variable climatic conditions. Consequently, the utilisation of radiant thermal management technology to reduce energy consumption and enhance living comfort has become an urgent priority [1–3]. Thermal radiation constitutes one of the three modes of heat transfer. All objects emit heat in the form of electromagnetic waves, with thermal radiation specifically denoting the phenomenon whereby objects radiate electromagnetic waves due to possessing a temperature. Consequently, any object with a temperature above absolute zero generates thermal radiation; the higher the temperature, the greater

the total energy radiated and the more pronounced the short-wave component. The Sun may be regarded as the most ideal and sustainable heat source. The sunlight it emits contains substantial light energy spanning ultraviolet, visible, and near-infrared wavelengths, alongside heat transfer between objects via mid-infrared radiation. However, the light and thermal energy delivered by solar radiation do not always align perfectly with human needs. To reduce energy consumption, radiative cooling technology has consequently emerged [4,5].

Static radiative cooling utilises outer space as the cold source for radiative heat exchange, achieving cooling by promoting radiative heat transfer through high emissivity in the mid-infrared atmospheric window band [6]. Currently, static radiative cooling primarily comprises transparent and non-transparent systems. Non-transparent coatings, utilising oxide particles such as titanium dioxide and silicon dioxide as primary materials, exhibit high reflectivity within the solar spectrum. These are chiefly applied to building facades and the surfaces of large heat-generating equipment [7–12]. Transparent radiative cooling systems, primarily fabricated from polydimethylsiloxane and materials rich in siloxane bonds, find applications in glass curtain walls, automotive sunroofs, and integration with solar cells and thermoelectric devices. For instance, when combined with solar cells, they simultaneously generate electricity while lowering photovoltaic panel temperatures, thereby enhancing photovoltaic conversion efficiency [13–18]. Additionally, by leveraging water vapor adsorption and desorption, solar radiation collection, and radiative cooling synergistic thermal effects, the temperature difference is amplified for thermoelectric power generation and atmospheric water harvesting [19,20]. However, static radiative cooling not only suffers from supercooling issues but also faces limitations in widespread adoption due to constraints on sustained cooling. The combination of phase change materials and static radiative cooling materials can harvest cold energy from the universe, regulating the surplus cold energy generated by nighttime remote control to compensate for the cold deficit during daytime remote control [21]. However, the extent of overcooling it can compensate remains limited. Consequently, dynamic radiative cooling has been extensively studied to broaden its application scope and unlock additional potential uses [22]. Researchers have observed that under ideal conditions, radiative cooling materials can achieve approximately 100 W/m^2 of radiative power within the atmospheric window band. However, practical applications may yield lower values due to various losses. The power density of energy contained within sunlight approaches 1000 W/m^2. Given the constraints imposed by energy thresholds regulated in the mid-infrared bands, dynamic control within the solar spectrum (visible-near infrared (VIS-NIR)) is crucial for reducing energy consumption [23–26].

Across the entire solar spectrum, VIS light (380–780 nm) accounts for nearly 43% of the energy content, with a power density approaching 500 W/ m^2. Dynamically adjusting the visible light transmittance to block heat gain in summer and retain warmth in winter significantly reduces building energy consumption, holding great importance for energy conservation [27,28]. Furthermore, dynamically regulating the proportion of different visible light colours within sunlight through functional films to control plant growth offers substantial application value for advancing agricultural technology [29]. NIR light (780–2500 nm) constitutes nearly 50% of solar energy. Its frequency aligns more closely with the resonant frequencies of microscopic particles within materials, conferring a stronger thermal effect. Consequently, dynamically regulating near-infrared transmittance in smart window applications holds substantial significance for reducing building energy consumption [30]. The mid-infrared (MIR, 2.5–25 μm) spectrum constitutes the primary band for inter-object heat transfer via thermal radiation. Particularly, the range of 8–13 μm is the transparent window

band of the atmosphere, which can be regarded as an ideal cold source for heat transfer between objects and outer space through this band, thereby achieving cooling effects. Dynamic regulation of this spectrum enables intelligent radiative cooling tailored to living requirements, holding substantial significance for reducing energy consumption [31–33]. Consequently, dynamically regulating the VIS-NIR-MIR tri-band spectrum to intelligently harness thermal radiation energy maximises energy savings, holding substantial implications for energy conservation and societal smart development. Dynamic thermal radiation management is transitioning from laboratory research to industrial implementation. Its interdisciplinary nature will reshape future landscapes across energy, electronics, aerospace and other sectors, establishing it as a pivotal technological pillar for carbon neutrality strategies. Several reviews have summarized dynamic radiative heat management research from perspectives including material systems [34], response mechanisms [35], and application scenarios [36]. However, analyses focusing on the principles of light behavior regulation remain scarce.

Therefore, this paper synthesised recent exemplary cases of light behaviour regulation, elucidating the principles and advantages of modulation across the visible, near-infrared, and mid-infrared regions from the perspectives of scattering, reflection, and light absorption. It further discussed light behaviour regulation tailored to application scenarios in both opaque and transparent systems (Figure 1). A clear understanding of the principles governing dynamic control across the visible, near-infrared, and mid-infrared bands enables optimisation of device performance for each specific band. This will facilitate more effective material and structural design tailored to defined application scenarios. Particular emphasis is placed on dynamic control for smart window applications within transparent systems, analysing optimal light behaviour regulation and outlining both the advantages and challenges associated with multi-band, multi-modal control. In summary, this review will provide researchers and industry professionals with comprehensive and up-to-date references, fostering further research and innovation in dynamic radiative thermal management technologies while guiding their practical implementation in industrial settings.

THE REGULATION PRINCIPLES OF EACH BAND

The visible, near-infrared, and mid-infrared bands not only exhibit significant differences in energy distribution, but their markedly distinct wavelengths necessitate fundamentally different principles for achieving dynamic regulation. The optical phenomena underpinning regulation in each band are not singular; typically, multiple phenomena coexist. Primarily, principles such as light reflection (Figure 2a), scattering (Figure 2b) and absorption (Figure 2c) are employed to dynamically regulate the transmittance of visible and near-infrared light, and to dynamically regulate the emissivity of the mid-infrared band [47–49]. Visible light serves dual functions of energy transfer and information exchange. For instance, in smart window applications, dynamic regulation of visible light transmittance must consider not only energy efficiency and daylighting but also fundamental window attributes such as visibility and visual comfort [50,51]. Consequently, a clear understanding of the principles governing dynamic modulation across the visible, near-infrared, and mid-infrared bands is paramount. This not only enables performance optimisation of devices tailored to each band but also facilitates more effective material and structural design for specific application scenarios [52]. Given that material interactions with the light field during dynamic switching states are

Figure 1 Overview of dynamic radiation thermal management (DRTM) systems [37–46]. Copyright©2025, John Wiley and Sons. Copyright©2017, Springer Nature. Copyright©2024, Elsevier. Copyright©2025, Royal Society of Chemistry. Copyright©2019, The American Association for the Advancement of Science. Copyright©2022, Springer Nature. Copyright©2023, John Wiley and Sons. Copyright©2024, Springer Nature. Copyright©2024, John Wiley and Sons. Copyright©2022, The American Association for the Advancement of Science.

multifaceted, we shall now focus on the mechanisms that play a dominant role in modulation.

Dynamic regulation of visible-light

The core technology of dynamically regulating visible light lies in altering a material's microstructure or electronic state through external stimuli (such as thermal, mechanical, optical, electrical, magnetic, or chemical inputs), thereby achieving dynamic modulation of its macroscopic transmittance (or reflectance) [41,53–57]. Different response mechanisms cause variations in the behaviour of incident light, leading to differences in the device's response speed, energy consumption, and durability, and corresponding to distinct specific application scenarios.

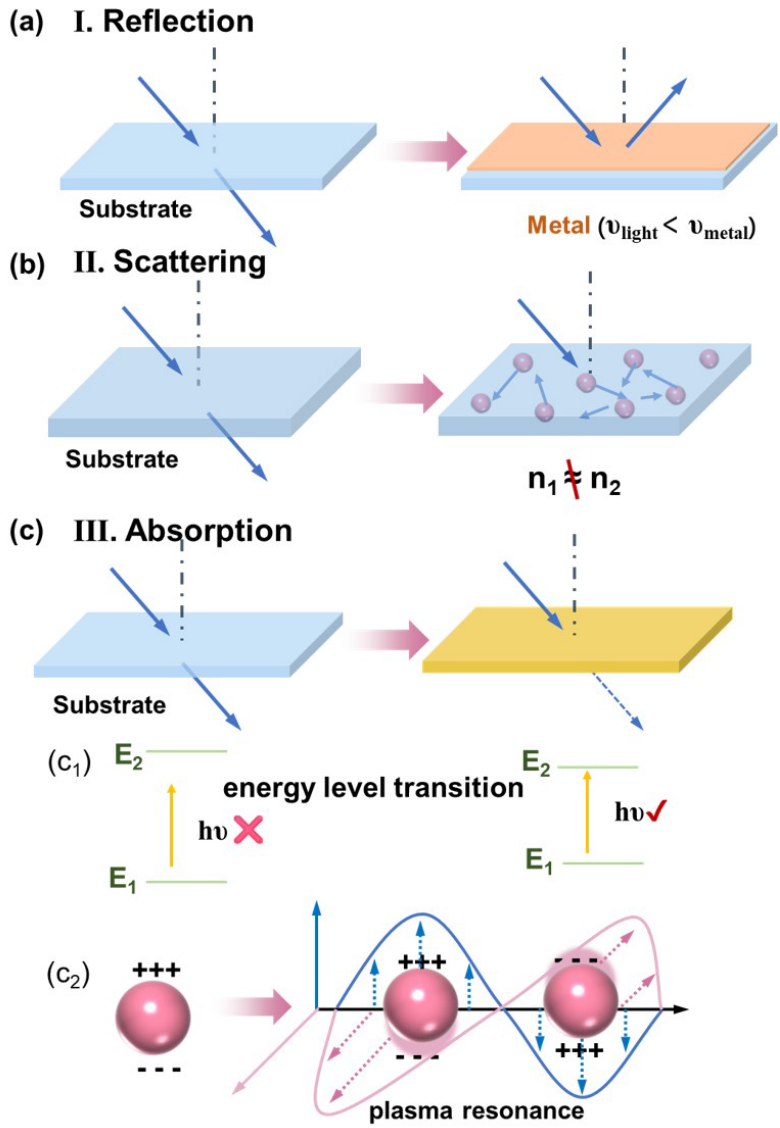

Figure 2 Schematic diagram of the principle of optical regulation. A schematic diagram illustrating the dynamic regulation of light reflection (a), light scattering (b) and light absorption (c).

Based on the reflection regulation of VIS

Structural design based on material intrinsic properties enables reversible transformations, utilising light reflection for adjustable radiative heat management applications. High reflectivity in the visible spectrum (approximately 400–700 nm) primarily involves electron interactions, band structure, and microstructural design [58]. For instance, in reversible metal electrodeposition systems, the presence or absence of a metallic layer alters light absorption and reflection, thereby effectively regulating transmittance. When light frequencies fall below the plasma frequency of metals, electrons respond rapidly to electromagnetic field changes, leading to high reflectivity, as observed in silver (Ag) and aluminium (Al) (Figure 2a) [59].

Therefore, by controlling the structure of the Ag layer, light reflection can be effectively regulated to achieve dynamic modulation (Figure 3a). For instance, visible light regulation is accomplished through the reversible electrodeposition of the Ag layer [57]. Through such structural design of the reversible silver layer's electrodeposition, the reflectance in the solar spectrum (0.3–2.5 μm) dynamically switches between 87.9% and 19.9% (Figure 3b) [60]. Inspired by cephalopod skin, an adaptive multispectral mechanical optical system was designed based on a bilayer acrylic dielectric elastomer (ADE)/silver nanowire (AgNW) film. This system reconfigures surface topography between wrinkles and cracks through mechanical contraction and stretching [61]. Silver nanowires deposited on the transparent elastomer upper layer exhibit a dramatic increase in inter-wire spacing during stretching, permitting greater light transmission and yielding high transmittance. Upon release of tension, the upper layer silver nanowires contract sharply under elastomeric action, inducing high reflectance and low transmittance, thereby effectively modulating visible light transparency. Similarly, coating silver nanowires onto polydimethylsiloxane (PDMS) surfaces enables the fabrication of flexible films with paper-cutout structures. Under tension, these structures expose macroscopic voids permitting visible light transmission. Upon tension release, the silver nanowires' high reflectivity reduces transparency, achieving dynamic switching [62]. Modulating visible light transmittance through light reflection primarily involves material structural design, leveraging silver's high reflectivity to achieve dynamic transparency switching. Furthermore, in dynamic radiative thermal management applications where aesthetic colour properties are considered, numerous material systems employ light reflection principles for dynamic colour switching, such as photonic crystals [63]. Within smart window applications, the advantage of modulating visible light via reflection lies in minimising solar energy intake during high-temperature phases. To some extent, this maximises the effective utilisation of modulated energy within thermal management research. However, this advantage carries a corresponding disadvantage: the intense specular reflection from silver layers may contribute to light pollution.

However, dynamic regulation achieved by exploiting light's diffuse reflection behaviour can effectively mitigate light pollution issues. Research on using diffuse reflection for dynamic transparency control remains scarce in the current literature. Through sequential strain release and multi-step oxygen plasma treatment, self-similar hierarchical wrinkles with nanoscale and micrometre-scale features were generated on pre-strained polydimethylsiloxane elastomers [56]. The layered wrinkled elastomer switched transparency states during repeated stretching and release cycles. This occurred because the micrometre-scale wrinkles on the pre-strained elastomer surface aggregated into a macroscopically rough surface, causing incident light to undergo diffuse reflection and thus appearing opaque. Upon tensile loading, the surface wrinkles effectively flatten, restoring transparency and thus enabling the transition. Diffuse reflection occurs when light scattered from a rough surface disperses uniformly in all directions. This arises because microscopic surface irregularities cause incident light to follow Fresnel reflection laws locally, yet manifest macroscopically as random directional scattering [64]. Light scattering, conversely, describes the deviation of light from its original path due to interactions with material constituents such as particles, defects, or density variations during propagation. This arises from interactions with microscopic or submicroscopic structures, encompassing both elastic scattering (where wavelength remains unchanged, e.g., Rayleigh scattering) and inelastic scattering (where wavelength shifts, e.g., Raman scattering) [65]. Diffuse reflection constitutes the statistical reflection behaviour of light upon macroscopically rough surfaces, whereas scattering arises from light's interaction with the internal structure of a medium. Both phenomena may coexist, yet their physical origins differ.

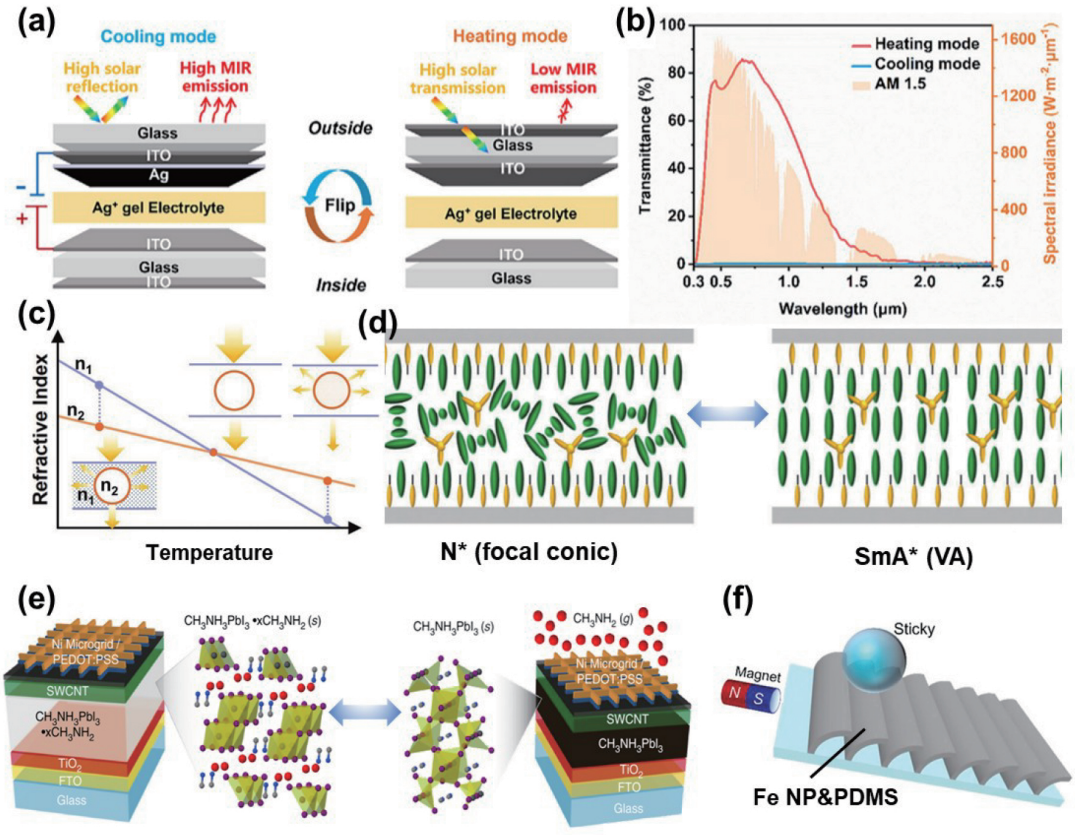

Figure 3 (a) The reversible metal electrodeposition of the silver layer regulates VIS [60]. (b) Spectra before and after silver layer deposition [60]. Copyright©2025, Wiley-VCH GmbH. (c) Schematic diagram of refractive index matching [66]. Copyright©2022, John Wiley and Sons. (d) The liquid crystal changes the orientation of its molecules under an electric field, and the effective refractive index also changes [67]. Copyright©2025, John Wiley and Sons. (e) Perovskite undergoes reversible coordination with methylamine, dynamically generating substances with strong visible light absorption [37]. Copyright©2017, Springer Nature. (f) The microplate structure containing Fe particles can be bent by magnetic field control [68]. Copyright©2023, John Wiley and Sons.

Based on the scattering regulation of VIS

Leveraging the characteristic of shorter wavelengths in visible light, optical scattering can effectively achieve dynamic regulation of visible light transmittance. This is accomplished by altering the microscopic structure of materials to modify their optical scattering behaviour before and after modification, thereby dynamically adjusting the visible light transmittance of thin films. The primary methods involve refractive index matching and crystal plane scattering control.

By utilising the principle of refractive index matching, the light scattering behaviour is controlled to regulate transmittance (Figure 3c). Paraffin wax, a classic phase-change energy storage material, has been applied in dynamic radiative thermal management research due to its phase-change temperature near room temperature, low cost, and excellent chemical stability [69]. For instance, when paraffin wax is combined with polyvinyl alcohol, based on the principle of refractive index matching, prior to paraffin wax phase transition, its refractive index approximates that of polyvinyl alcohol, yielding high film transmittance. Upon temperature elevation, paraffin wax undergoes a phase transition from solid to liquid state, altering its refractive index. This discrepancy with polyvinyl alcohol's refractive index induces high scattering of

shorter-wavelength incident light [46]. Thus, through temperature control, dynamic regulation of the film's transmittance is achieved based on light scattering behaviour [70]. Similarly, the phase-change material eicosane was deposited onto polyurethane nanofibres via electrospray technology. Upon reaching 37 °C, eicosane rapidly undergoes phase transition. Post-transition, its refractive index approximates that of the outer polyurethane layer, establishing optical transmission pathways between nanofibres and preventing light scattering loss at nanofibre-air interfaces [71]. Similarly, employing a one-step emulsification method to embed ethylene glycol solution droplets within polydimethylsiloxane (PDMS) yielded an adaptive thermoresponsive smart window based on dynamic refractive index (RI) matching between two phases, achieving intelligent temperature response in PDMS [66]. The principle of achieving dynamic visible light regulation in hydrogel material systems is analogous, all involving control through the occurrence of light scattering behaviour [55]. For instance, poly(*N*-isopropyl acrylamide) (PNIPAm), typically synthesised via radical polymerisation, exhibits a curl-to-ball transition in polymer chains [72]. Additionally, thermoresponsive micelles are incorporated into highly transparent hydrogel matrices, where micelles undergo reversible aggregation and dissociation in response to temperature changes [73]. In all these material systems, external thermal field stimulation induces changes in the internal microstructure, controlling light scattering behaviour to achieve effective dynamic regulation of visible light transmittance. Furthermore, by applying external force fields to stimulate its structure to undergo reversible changes, the refractive index can be regulated, thereby altering the light scattering behavior [74], such as fabricating a wrinkled structure on the top surface of an elastomeric polydimethylsiloxane film, embedding silica particles within the film substrate, thereby constituting an on-demand mechanically responsive smart window [75–77]. The principle governing visible light regulation involves the generation of secondary wrinkles and nanoscale voids around the particles during external force application (i.e., stretching). The refractive mismatch between these voids and the silica particles induces intense light scattering upon visible light incidence, thereby reducing film transmittance and dynamically modulating light scattering behaviour.

Similarly, the visible light transmittance of dynamically regulated films is often effectively controlled through solvent stimulation by exploiting light scattering behaviour [78]. For instance, a solvent-activated colour-changing hydrogel for self-protective smart windows was developed using the structural design of cellulose-polyacrylamide supramolecular assemblies [41]. When exposed to an ethanol molecular environment, this gel adsorbs ethanol molecules, inducing a conformational change in its supramolecular structure. Here, polyacrylamide (PAAm) molecules wrap around cellulose chains via hydrogen bonds. As ethanol molecules guide incident light through this structure, the alcohol gel exhibits high transmittance in this state. However, upon thermal volatilisation and escape of ethanol molecules from the gel, the exposed compact supramolecular structure tends to scatter most incident light, exhibiting pure white opacity with low transmittance. This solvent-induced colour-changing alcohol gel utilises light scattering principles to achieve dynamic switching between transparent and opaque states. This work similarly presented results for methanol and acetone stimuli, operating on identical principles. Beyond methanol, ethanol, and acetone molecules responding to stimuli, water molecules were also commonly employed as stimulus molecules in current research [79,80]. Across various chemical stimuli, the underlying modulation principle fundamentally leverages light scattering to effectively regulate visible light.

Furthermore, regulation is achieved through the scattering of crystal planes within the material's internal crystalline structure (Figure 3d). Liquid crystal systems, for instance, represent a typical material system that

dynamically modulates visible light transparency via light scattering. Owing to the optical anisotropy of liquid crystals and the dependence of their optical properties on molecular orientation, precise control over the arrangement of liquid crystal molecules is attained by applying external stimuli, thereby regulating their optical state [81]. For instance, in chiral liquid crystals, the three-dimensional molecular orientation of the chiral liquid crystal (LC) is adjusted via external stimuli (light or heat). This orientation is autonomously controlled within the host liquid crystal (HLC) through surface molecular engineering based on azobenzene and bulk molecular engineering [67]. Chiral liquid crystals exhibit transparency in their initial state due to the vertical alignment of host liquid crystals within chiral metamorphic phase A (SmA*) monolayers. Upon intense ultraviolet irradiation, photoisomerised azobenzene-based ordering molecules transform the SmA* single domain into randomly dispersed multiple domains, inducing strong light scattering and transitioning to an opaque state, thereby achieving dynamic transparency control. Furthermore, an electric field can drive the rearrangement of liquid crystal molecules, altering their photofield-modulation effects and enabling transparency switching [82,83]. High-temperature-induced phase transitions in liquid crystal materials from one nematic phase to another result in alterations to texture and light-scattering capability. In cholesteric liquid crystals, successive cholesteric LC layers shift through minor rotations of the molecular orientation vector relative to adjacent layers [84]. Under an electric field, high haze is achieved by controlling the arrangement of liquid crystal molecules to modulate light scattering, thereby regulating transparency. Modulating visible light transmittance through light scattering primarily relies on principles such as refractive index matching, reversible changes in microstructure, and molecular rearrangement to generate high haze [81]. In smart window applications, light scattering modulation offers the advantage of structural simplicity. Moreover, the generation of high haze enables privacy protection while maintaining normal daylight transmission.

Based on the absorption regulation of VIS

The essence of visible light absorption lies in the conversion of photon energy into the excited-state energy of a material through mechanisms such as electron transitions (interband/intraband), plasmon resonance, or charge transfer [85]. The specific pathways are jointly determined by the material's electronic structure, chemical composition, and microstructure [86,87]. Through structural design enabling reversible changes, the absorption of visible light can be altered, thereby achieving dynamic regulation of thermal radiation for effective thermal management.

Firstly, light absorption arises from energy level transitions, which depend on the intrinsic properties of the material itself (Figure 2c$_1$). Consequently, dynamic regulation can be achieved by dynamically generating substances with strong visible light absorption (Figure 3e). For instance, adaptive PDRC materials utilising thermosensitive phase transitions based on amorphous calcium carbonate (ACC) and thermochromic microparticles (TMP) exhibit significant alterations in light absorption due to the reversible formation and disruption of conjugated regions within the TMP chromophore molecules. Specifically, the chromophore loses electrons and opens the ring, forming a conjugated structure and assuming a coloured state to efficiently store heat at low temperatures. Conversely, upon electron gain, the chromophore closes the lactone ring to produce a white state, facilitating radiative cooling at elevated temperatures [88]. Perovskite materials, for instance, have been extensively developed as smart window photovoltaic materials owing to their straightforward, cost-effective synthesis and superior optical properties [89,90]. Temperature variations

trigger reversible hydration/dehydration reactions, altering their crystal structure and light absorption to effectively modulate visible light transmittance [91]. At lower temperatures, perovskite exists as a dihydrate ($MA_4PbX_6 \cdot 2H_2O$) with a loose crystal structure, where water molecules are embedded within the lattice. This results in weak light absorption and a transparent state for the material. Upon heating to a critical point (e.g., 45 °C), the perovskite undergoes dehydration, losing bound water molecules and transforming into a compact $MAPbX_3$ crystal structure. This structural change significantly enhances visible light absorption, causing the material to turn reddish-brown (Figure 3e) [92]. Beyond hydration/dehydration regulation, perovskite systems can also undergo colour change through the complexation/dissociation of methylamine [37]. Furthermore, by alloying the perovskite and employing dimethyl sulfoxide (DMSO) as an inducer for temperature-controlled colouration/decolouration regulation, distinct red, yellow, and brown hues have been achieved [93]. Additionally, temperature control alters the periodically arranged structure within the photonic crystal, thereby modifying light absorption. This enables multicolouration while simultaneously facilitating effective radiative thermal management [94].

Most photochromic materials generate new substances through changes in valence states, bond breaking and formation, and molecular isomerisation, thereby exhibiting strong visible light absorption and enabling regulation. Examples include inorganic photochromic materials such as tungsten oxide, titanium dioxide, and silver halides [95,96]. Under intense ultraviolet irradiation, tungsten oxide generates abundant electrons and holes, forming tungsten bronze (pentavalent tungsten) that induces colouration and strong light absorption [54]. Similarly, titanium dioxide operates on a comparable principle: ultraviolet excitation creates Ti^{3+} defect states that absorb visible light [97]. Silver halides function through photon energy reducing Ag^+ to Ag atoms (nanoclusters), where localised surface plasmon resonance (LSPR) within Ag particles enhances visible light absorption [95]. Furthermore, by immobilising BiOCl nanosheets within a calcium alginate (CA) hydrogel matrix, light-triggered oxygen vacancy accumulation promotes electron localisation at Bi sites, weakening Bi–O bonds to drive photochromism. This mechanism alters light absorption through Bi surface plasmon resonance (SPR) and c-induced bandgap narrowing [98]. Numerous studies have documented the application of organic photochromic materials in energy-saving smart windows, including spiropyran derivatives and azobenzene compounds [99]. Photchromic materials such as spiropyran derivatives, e.g., 3′,3′-dimethyl-6-nitro-spirocyclohexane, exhibit a distinct transition from violet to colourless under illumination. This occurs due to C–O bond cleavage under UV irradiation, leading to molecular planarisation, expansion of the conjugated system, and shifts in absorption peaks, resulting in violet colouration [100]. Beyond bond cleavage, colour-changing principles in organic photochromic materials may also be achieved through reversible molecular isomerisation. This alters absorption peaks, enabling simultaneous colouration and dynamic regulation of visible light transmittance. For instance, azobenzene derivatives undergo *cis*/*trans* photoisomerisation, modifying their visible absorption spectra [101]. Owing to the photoresponsive stability of azobenzene derivatives, they are typically integrated with static radiative cooling materials for application in dynamic radiative thermal management [102].

Moreover, the reasons for the strong absorption of substances in visible light are not singular. Beyond absorption arising from energy level transitions, absorption often occurs due to plasmon resonance, which is closely related to carrier concentration (Figure $2c_2$). For instance, in classic transition metal oxide systems used in electrochromic materials, such as the cathodic colour-changing layer of tungsten oxide and the anodic colour-changing layer of nickel oxide [103]. Upon application of a negative voltage, electrons (e^-) and

cations (such as H^+, Li^+, and Al^{3+}) are injected into WO_3. W^{6+} is reduced to W^{5+}, forming polaritons ($W^{5+} \leftrightarrow W^{6+}e^-$). Electron localisation leads to visible light absorption (blue). Under reverse voltage, cations and e^- are desorbed, restoring transparency. For anodic colour-changing nickel oxide layers, the mechanism is analogous. Under electric field influence, Ni^{2+} oxidises to Ni^{3+}, accompanied by OH^- deprotonation, transforming transparent $Ni(OH)_2$ into NiOOH (dark brown), thereby altering light absorption. Reversible metal electrodeposition (e.g., copper [104], zinc [105], manganese dioxide [106]) enables strong visible light absorption by controlling the dissolution and deposition of the metal layer, thereby allowing effective regulation of visible light. For conductive polymer systems like polyaniline, monocomponent organic polymer polyaniline (PANI) exhibits photoconversion capability. Through progressive electrochemical reactions, PANI films demonstrate remarkable electrochromic properties of rich colour transitions (yellow-green-black). The colour-changing mechanism involves multi-step oxidation state changes under electric fields, altering π-π* transition energy. Different oxidation states result in multiple PANI states, concurrently altering light absorption and thus enabling colour switching [107]. Similarly, polythiophene derivatives like poly(3,4-ethylenedioxythiophene) achieve transparency-to-blue switching through electrochemical doping/dedoping, which modifies polariton absorption in the conjugated chain. Research indicates that incorporating conductive liquid gallium nanoparticles (GaNPs) into poly(3,4-ethylenedioxythiophene):poly-(styrenesulfonate) (PEDOT:PSS) enhances electrochromic performance. The liquid state of GaNPs facilitates rapid oxidation and reduction of the interfacial gallium oxide layer. Moreover, the crack structure within the oxide layer enables swift carrier exchange while permitting efficient charge storage within the oxide matrix [108]. Prussian blue analogues (MTHCF) constitute a class of open-framework compounds formed by 'FeII–C≡N–MT' units, with Prussian blue (FeHCF, MT=Fe) being the most renowned example. FeHCF films exhibit reversible blue-to-colourless transitions under applied voltage. This colour change arises from charge transfer between Fe^{3+} and Fe^{2+} ions under electric fields, altering their valence states and inducing decolourisation. Their non-toxicity, straightforward preparation process, and scalability for large-area fabrication have driven extensive research [109]. Beyond this, compounds such as azurines undergo multi-step reduction reactions accompanied by radical formation and π-π* transitions, thereby altering light absorption and inducing colour changes for visible light regulation [110]. Electrochromic materials alter light absorption properties through electric field-driven ion/electron transfer (e.g., polariton formation in WO_3) or redox reactions (e.g., single-electron reduction in violet dyes). Inorganic materials (WO_3, NiO) offer high stability, organic materials (PANI, violet dyes) provide rapid response, while hybrid systems combine the advantages of both.

Furthermore, dynamic regulation is achieved not by altering the material's intrinsic light absorption properties, but by dynamically switching its microstructure to control light absorption behaviour (Figure 3f). Microplate array structures fabricated from shape memory alloys bend upon temperature control, causing the microplates to obstruct light transmission pathways. This induces strong absorption of incident light, thereby reducing transmittance [111,112]. Alternatively, magnetic fields control the microplate array by incorporating strong visible-light-absorbing magnetic particles such as Fe [53,68], Ni [113], or Fe_3O_4 [94]. Magnetic field-induced bending of the microplates, combined with the strong light absorption of metallic Fe particles, enables switching of visible-light transparency (Figure 3f) [53]. One-dimensional (1D) superparamagnetic Fe_3O_4@SiO_2 nanorods exhibit a visible light transmission pathway when aligned parallel to the observation direction under a magnetic field, presenting a transparent state. Upon magnetic field removal, the

randomly oriented nanorods strongly absorb visible light, enabling dynamic switching [114].

In summary, modulating visible light through altered light absorption offers significant advantages over scattering and reflection. Within smart window applications, dynamically controlling visible light via absorption first reduces haze formation, safeguarding fundamental window visibility while diminishing glare and enhancing visual comfort. Secondly, energy harvesting through absorption enables multifunctional device integration, such as photovoltaic-electrochromic coupling; It delivers glare-free environments, eliminating visual interference. Smart dimming technology based on light absorption regulation, through dynamic solar radiation management, optimised energy efficiency, and enhanced user experience, emerges as a core solution for green buildings and smart terminals. Its fundamental advantage lies in transforming passive materials into actively controllable optical systems, combining functionality, cost-effectiveness, and sustainability. This positions it as a pivotal technology for future smart cities.

Dynamic regulation of near-infrared

Research into achieving energy efficiency and thermal comfort by modulating transmittance in the NIR (700–2500 nm) band has primarily focused on three mechanisms: light reflection, scattering, and absorption. Given that both light scattering and diffuse reflection exhibit strong wavelength dependence, the modulation efficiency for achieving dynamic control of the near-infrared band through these means is significantly inferior to that achievable in the visible spectrum. Moreover, whilst dynamically regulating the near-infrared band through light scattering and diffuse reflection, visible light regulation is inevitably achieved simultaneously, with visible light regulation taking precedence over the near-infrared band. This approach severely limits multi-band, multi-level regulation.

Based on scattering and reflection regulation of NIR

The principle of controlling near-infrared light through light scattering regulation is identical to that of visible light regulation discussed previously. However, due to its strong wavelength dependency and the fact that near-infrared wavelengths are longer than visible light, it exhibits greater penetration capability at the macroscopic level, thereby limiting its modulation potential. For instance, by employing the principle of refractive index matching, the intensity of light scattering by thin films can be dynamically altered through temperature control, enabling dynamic switching of near-infrared transmittance (Figure 3c) [115,116]. In the classic hydrogel material system utilising light scattering regulation, broad and intense absorption bands arise from the overtones and combination bands of the O–H bond stretching and bending vibrations of water molecules. particularly peaking at 1400–1500 nm and 1900–2000 nm. Additionally, overtones and combination bands from C–H bond vibrations in the polymer network contribute to NIR absorption, thereby limiting hydrogel's dynamic modulation rate in the near-infrared spectrum [117]. Similarly, the liquid crystal systems previously described for modulating visible light via light scattering can also concurrently regulate the near-infrared band. For instance, transparent poly (stearoyl acrylate) (poly (SA)), termed CPSA, comprises poly (SA) and ethoxylated trimethylolpropane triacrylate. UV curing at elevated temperatures suppresses microcrystalline domain size to the nanometre scale, achieving high optical transparency and crystallinity at ambient temperatures. The refractive index of the poly(HEMA) phase is adjusted to match that

of the CPSA phase, rendering the terpolymer film transparent at 20 °C with visible light transmittance reaching 91.4%. Above the transition temperature of 42–46 °C, melting of CPSA crystals causes light scattering at the phase interface, resulting in an opaque appearance [118]. Spectral analysis reveals that modulation amplitude diminishes with increasing wavelength. Systems employing light scattering and diffuse reflection for dynamic regulation, such as those responding to solvent molecules or mechanically altering internal microstructures, enable concurrent control across visible and near-infrared wavelengths (Figure 2b).

Beyond the reversible deposition of metallic layers previously discussed (Figure 3a), the regulation of near-infrared wavelengths through light reflection primarily relies on two mechanisms: plasmon resonance and free carriers (Figure 2c). Both fundamentally alter a material's optical absorption properties, accompanied by changes in reflectance. First, localised surface plasmon resonance (LSPR) occurs when free electrons within nanostructures (such as indium tin oxide (ITO) nanocrystals or gold nanorods) undergo collective oscillation under the influence of near-infrared electric fields, forming plasmonic resonance. This phenomenon also induces intense reflection/scattering at specific wavelengths [119]. For instance, a nanostructure comprising ITO nanoparticles and polythiophene nanoparticles/polymer exhibits electrochromic behaviour, demonstrating promising characteristics where infrared (IR) transmission above 800 nm can be reversibly controlled by applying merely 1.25 V. [120] However, substantial absorption occurs within the visible spectrum, thus limiting this system's transmittance to visible wavelengths. Secondly, free carrier modulation involves altering the concentration of free carriers (electrons/holes) within the material via electric fields or chemical doping, thereby adjusting its plasmon frequency (ω_p) to modify near-infrared reflectance. For instance, lithium ion intercalation into WO_3 increases conduction band electron concentration, elevating near-infrared reflectance [121]. Additionally, reversible metal electrodeposition systems achieve dynamic regulation through the deposition and dissolution of Ag layers [122,123]. However, the limited near-infrared transmittance of the ITO/FTO (fluorine-doped tin oxide) electrode layer restricts the modulation range within this spectral band. Furthermore, alternating deposition of high- and low-refractive-index media (e.g., TiO_2/SiO_2) creates photonic bandgaps, inducing Bragg reflection to selectively reflect near-infrared light. This is achieved by varying the interlayer spacing [124]. Nevertheless, such approaches predominantly involve static structural design.

Based on the absorption regulation of NIR

Localised surface plasmon resonance (LSPR) may manifest as either strong scattering/reflection or strong absorption in response to incident light, with the specific behaviour dependent upon the material, size, morphology, and surrounding dielectric environment of the nanoparticles [125]. LSPR constitutes a collective oscillation phenomenon of free electrons within metallic or doped semiconductor nanoparticles under the influence of an electric field [48]. When the incident light frequency matches the intrinsic oscillation frequency (plasmon frequency) of the electron cloud, a resonance effect occurs, significantly enhancing light-matter interaction (Figure 3c). When the LSPR frequency of nanostructures falls within the near-infrared region, strong absorption is generated [126]. Consequently, the LSPR peak position can be dynamically tuned by altering nanoparticle shape, size, or the surrounding dielectric environment (e.g., through electrochemical redox processes) [127,128]. For instance, in VO_2 nanopowders, a phase transition occurs

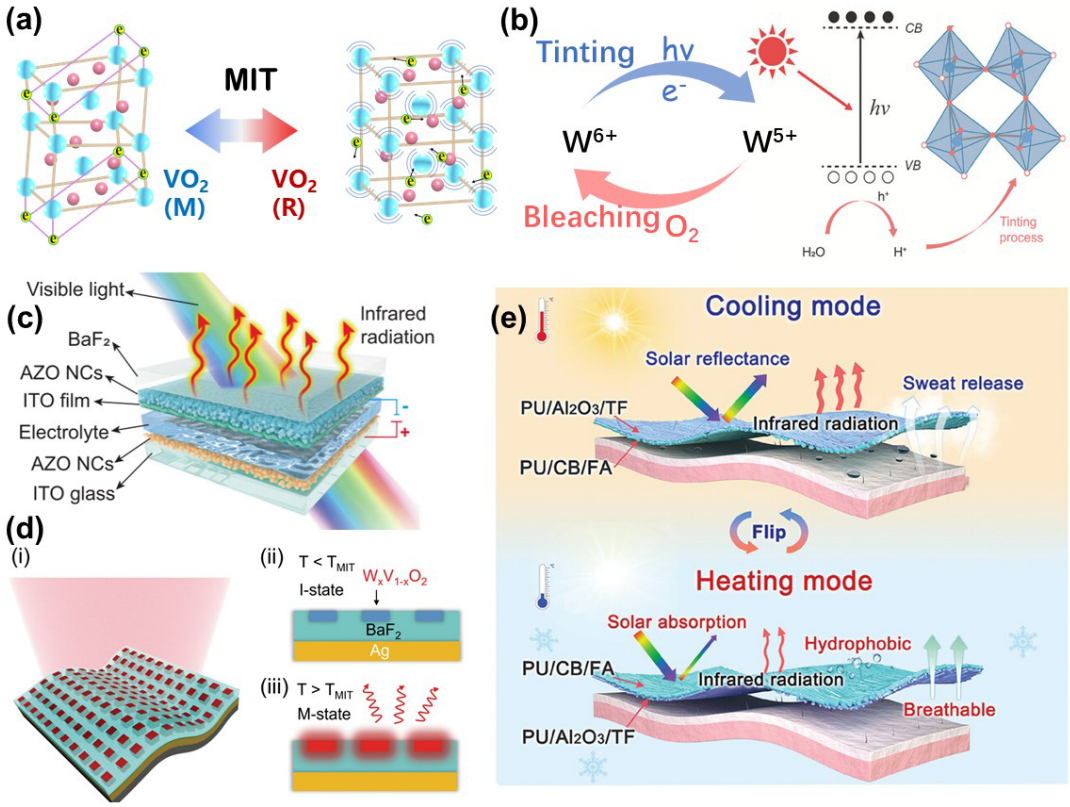

Figure 4 (a) Vanadium dioxide temperature-controlled switching structure undergoes phase transition to regulate near-infrared radiation. (b) The mechanism of regulating the photochromic tungsten oxide under near-infrared light [54]. Copyright©2024, John Wiley and Sons. (c) Dynamic regulation of the emission rate of mid-infrared in aluminum-doped zinc oxide nanocrystals (AZO NCs) [132]. Copyright©2023, Springer Nature. (d) Dynamic regulation of mid-infrared emissivity in F-P cavity structure based on phase-change material VO_2 [133]. Copyright©2021, The American Association for the Advancement of Science. (e) The Janus structure regulates the mid-to-long infrared emissivity through mechanical flipping [134]. Copyright©2024, John Wiley and Sons.

above 68 °C, transforming the material from an insulating to a metallic state with increased carrier concentration. The strong absorption observed in the transmission spectrum of VO_2 nanopowders near 1400 nm stems from resonance absorption induced by the LSPR effect (Figure 4a) [129].

Moreover, absorption in the near-infrared band also relies on free carrier absorption [130]. Free electrons within the material undergo collision-damped motion under the influence of a near-infrared electric field, absorbing photon energy and converting it into Joule heat. For instance, in the classic electrochromic tungsten oxide system, lithium ions become embedded within the WO_3 layer upon voltage application. This increases the conduction band electron concentration, enhancing free carrier absorption and consequently reducing near-infrared transmittance [131]. Similarly, in reversible metal electrodeposition systems, such as those employing copper [104], zinc [105], manganese dioxide [106], exhibit heightened free carrier concentrations and enhanced absorption. Conversely, in photochromic tungsten oxide systems, ultraviolet irradiation induces electron-hole pair generation, with some electrons captured by W^{6+} to form W^{5+}. The W^{5+} defect state generates subbandgap absorption in the near-infrared region, thereby diminishing transmittance in this wavelength band (Figure 4b) [54].

The principles governing the dynamic regulation of VIS and NIR light absorption through light absorption share commonalities yet exhibit significant differences. Strong near-infrared absorption primarily relies on the material's optical bandgap, charge carrier behaviour, or molecular vibrational characteristics. Strong near-infrared absorption is mainly achieved through free charge carriers, narrow bandgap transitions, or molecular vibrations, whereas visible light absorption depends on electron bandgap transitions.

Dynamic regulation of mid-infrared

The ratio of the energy radiated by a material at a specific temperature to the energy radiated by a blackbody at the same temperature (where $\varepsilon = 1$ denotes an ideal blackbody and $\varepsilon = 0$ denotes a perfect reflector) is defined as the material's emissivity. Kirchhoff's law states that for objects in thermodynamic equilibrium, the spectral emissivity ($\epsilon\lambda$) equals the spectral absorptivity ($\alpha\lambda$): $\epsilon\lambda = \alpha\lambda$. This relationship holds for all wavelengths (including the mid-infrared band) and all directions [39]. The core principle of dynamically regulating mid-infrared (5–25 μm) emissivity involves inducing reversible changes in materials or structures to alter their surface interaction with thermal radiation, thereby enabling intelligent control over thermal radiation dissipation or absorption.

The principle of modulating carrier concentration (plasmonic effect) is employed to regulate emissivity in the mid-infrared spectrum (Figure 2c). This involves altering the material's free carrier concentration (n) through external stimuli (electric fields, chemical doping), thereby controlling its plasmonic frequency (ω_p) and consequently influencing mid-infrared reflection or absorption characteristics [132,135,136]. When the incident light frequency $\omega < \omega_p$, the material exhibits high reflectivity; when $\omega > \omega_p$, it behaves as transparent or absorptive.

Aluminium-doped zinc oxide (AZO) nanocrystals exhibit distinct absorption characteristics in the mid-infrared region due to variations in local surface plasmon resonance absorption intensity (Figure 4c). This is caused by electron injection/extraction within the depletion layer at the AZO nanocrystal surface under electric field control. Consequently, their mid-infrared emissivity is dynamically regulated (0.51 at 3–5 μm and 0.41 at 7.5–13 μm) [137]. Following lithium-ion intercalation, the carrier concentration within WO_3 electrochromic films increases, causing a significant alteration in mid-infrared reflectance and thereby modulating the mid-infrared emissivity [138,139]. Electrodes based on IR-transparent graphene enable the development of dynamic IR emissivity modulation devices through the reversible electrodeposition of metals onto graphene-based electrodes [140]. Within reversible metal electrodeposition systems, infrared radiation can be dynamically modulated through the reversible electrodeposition and dissolution of silver layers [141].

By exploiting the principle of metal-insulator phase transitions (abrupt changes in electronic structure) to modulate mid-infrared bands [142], namely the drastic alteration in electron density during material phase transitions, which causes a reversal in mid-infrared optical properties (Figure 4d) [143]. For instance, employing the classic thermally controlled phase-transition material VO_2, the insulating phase (vanadium dioxide) exhibits high mid-infrared absorption, whereas the metallic phase demonstrates high mid-infrared reflectivity, thereby enabling emissivity modulation [144]. Similarly, hydrogen-induced metal-insulator transitions in Mg_xNi alloy films enable their use as variable-emissivity materials and top conductive electrodes [145]. Polyethyleneimine (PEI) serves as the intermediate proton-conducting electrolyte layer, while hydrogen-tungsten bronze (H_xWO_3)/ITO forms the bottom ion storage layer. The constructed sandwich-

structured electrochromic device simplifies the device architecture while ensuring substantial emissivity variation. This introduces a novel approach for dynamic emissivity modulation based on hydrogen-induced metal-insulator phase transitions from metallic yttrium (or yttrium dihydride) to dielectric yttrium trihydride, utilising yttrium/rhodium metal films and infrared-transparent cover layers [146]. By alternately injecting a 4% hydrogen-argon mixture and air into the gas-chromatographic device, its infrared emissivity is dynamically and reversibly modulated. The essence of dynamically regulating mid-infrared emissivity lies in actively altering the material's 'absorption-reflection' equilibrium for thermal radiation through electronic behaviour (charge carriers, phase transitions), photonic structures (metasurfaces), or molecular vibrations.

Furthermore, studies have reported the utilisation of Janus surfaces to modulate mid-infrared emissivity (Figure 4e) [147–149]. Materials featuring upper and lower layers with high mid-infrared emissivity and high reflectivity (low emissivity), respectively, enable dynamic emission control by mechanically flipping the material's top layer to face the sky. As reported, one surface is coated with a hydrophobic polymer cooling layer comprising micro/nanoporous/particle layered structures, while the other surface is coated with hydrophilic MXene nanosheets for heating. The cooling surface exhibits high solar reflectance (96.3%) and infrared emissivity (95.5%), resulting in sub-ambient radiative cooling during both day and night. Conversely, the heating surface demonstrates high solar absorptance (83.7%) and low infrared emissivity (15.2%) [147]. This control mechanism does not involve smart materials; instead, dynamic regulation is achieved through the mechanical flipping of static materials.

THERMAL MANAGEMENT APPLICATIONS IN TRANSPARENT AND NON-TRANSPARENT SYSTEMS BASED ON DTRC

Having understood the principles of dynamically regulating VIS, NIR, and MIR through light reflection, scattering, and absorption, along with existing response mechanisms and commonly used material systems, we can better design, optimise, and modify materials according to our specific requirements. Coupled with the performance advantages brought by current device integration, dynamic radiative thermal management is evolving towards energy efficiency, intelligence, and high performance. Dynamic radiative thermal management adapts to environmental temperature fluctuations or operational requirements by real-time regulation of a material or system's transmittance across the solar spectrum (350–2500 nm) and its emissivity characteristics in the mid-infrared bands. Its core lies in employing dynamically tunable materials or structures to switch transmittance through the solar spectrum and mid-infrared emissivity, thereby achieving efficient thermal control. Based on application scenarios, dynamic radiative thermal management broadly falls into two categories: non-transparent systems and transparent systems. The primary distinction lies in controllable high transmittance within the visible light spectrum.

Non-transparent system

Numerous studies have documented thermal management applications in non-transparent systems, such as radiative cooling technologies. However, their static spectral response leads to supercooling issues. Consequently, to further reduce energy consumption, the application of dynamic radiative thermal management

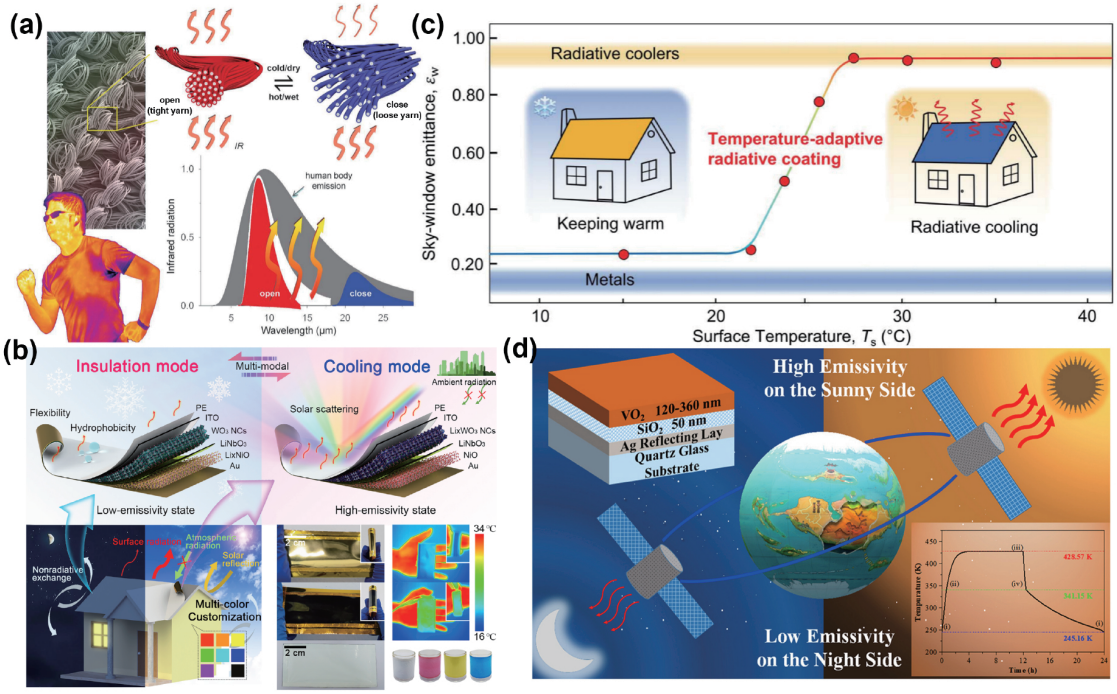

Figure 5 Radiant thermal management applications in non-transparent systems, personal thermal management [39] (a) (Copyright©2019, The American Association for the Advancement of Science), building walls ((b) [138] and (c) [133]) (Copyright©2025, John Wiley and Sons; Copyright©2021, The American Association for the Advancement of Science), and space thermal management [150] (d) (Copyright©2022, Elsevier).

in non-transparent systems requires further development. Dynamic radiative thermal management for non-transparent systems represents a cross-disciplinary breakthrough spanning thermal science, materials science, and engineering. Its applications permeate scenarios from everyday life to cutting-edge technology, encompassing smart textiles, electronic heat dissipation, building energy efficiency, aerospace, military camouflage, and industrial thermal control (Figure 5). Owing to its significant energy-saving potential, performance enhancements, and strategic value, coupled with advancements in new materials and intelligent algorithms, dynamic radiative heat management technology is poised to become a core technology for future green energy, high-performance computing, and national defence security.

Personal thermal management

Thermal radiation constitutes the primary mode of heat transfer and serves as an effective means of regulating heat exchange between the human body and its environment. The appropriate and efficient application of thermal radiation within personal thermal management textiles enhances individual thermal comfort while offering significant benefits for energy conservation. In the realm of personal thermal management, adaptability is primarily achieved by modulating the absorption rate within the solar spectrum and the emissivity in the mid-infrared range. This is complemented by synergistic regulation through heat conduction, convection, and evaporative cooling mechanisms [151]. Consequently, with the growing demand for multifunctional human textiles in daily life, the research and development of functional textiles holds

significant importance [152,153]. Humans are homeothermic creatures. Excessively low temperatures impair enzymatic activity and normal metabolic processes, potentially leading to fatal outcomes. However, the limited thermal regulation capabilities of conventional textiles make it challenging for individuals exposed to outdoor environments to maintain stable body temperatures. Consequently, exploring novel smart textiles for dynamic thermal management holds significant practical value [154].

Consequently, extensive research has been reported on intelligent textiles exhibiting dynamic thermal management capabilities [152]. For instance, adaptive thermal management integrates both heating and cooling functions within a single fabric, featuring passive reflective cooling derived from a photonic crystal (PC) layer and active heating via a nano-silver layer driven by voltage [155]. The art of personal thermal management lies in effectively mitigating thermal stress by manipulating the target object's spectral properties. However, improvements remain necessary in developing structures capable of seamlessly adapting to diverse thermal environments. Addressing this challenge, researchers have engineered Janus-surface fabrics, which, when meticulously designed, offer unique advantages for multi-scenario applications. A Janus fabric exhibiting 92% solar reflectance and 94% emissivity on its upper surface, coupled with an infrared emissivity below 30% on its underside, facilitates adaptive thermal management. This configuration enables self-selection of the outer layer based on ambient temperature conditions, with the upper side dissipating heat and the lower side retaining warmth [152]. Similarly, Yin *et al*.'s [156] dual-mode Janus-structured fabric offers both radiative cooling and solar heating. This structure demonstrates strong adaptability across diverse climatic conditions. Furthermore, scalable manufacturing compatibility and outstanding performance position Janus structures as a promising avenue for various passive thermal management scenarios. Additionally, reports have combined dynamic bidirectional thermal regulation of Janus structures with unidirectional sweat transport to achieve more efficient personal thermal management [157–159]. For instance, the cooling side features an *in-situ* grown nano-ZnO layer, achieving high solar reflectance and infrared emissivity. The heating side, functionalised with PDMS@rGO (reduced graphene oxide) composites, exhibits significant solar absorption and unidirectional moisture transport through hydrophilic-hydrophobic interactions. Furthermore, integrating thermal radiation regulation with phase change energy storage enables efficient personal thermal management. As exemplified by the proposed temperature-adaptive Janus phase-change radiative cooling fabric, electrostatic spinning integrates a radiative cooling layer (PVDF-HFP) with a phase-change material layer (PEG) to fabricate a temperature-adaptive phase-change radiative cooling textile [160]. The radiative cooling layer effectively reflects and scatters the entire solar spectrum while emitting thermal radiation within the atmospheric window. The phase change material layer dynamically provides temperature-adaptive cooling or heating compensation for the radiative cooling effect.

Moreover, by constructing an infrared-adaptive textile composed of polymer fibres coated with carbon nanotubes, the yarn itself expands and collapses in response to heat and humidity. This alters the spacing between fibres, thereby modifying the textile's infrared emissivity (Figure 5a) [39]. Similarly, by regulating the yarn twist morphology and coil-helix chirality within a textile multistage structure, a 'super-louver' fabric with moisture-responsive pore modulation was designed, enabling all-weather thermal-humidity regulation in smart textiles [161]. Dynamic thermal control was achieved by controlling the opening and closing of pore channels [162]. Building upon the principle of dynamically modulating emissivity, research demonstrates the fabrication of dynamically temperature-regulating textiles by weaving scalable radiative electrochromic fibres. Driven by low voltage, these fibres exhibit modulated mid-infrared emissivity with $\Delta\varepsilon \approx 0.35$, enabling

effective thermal management [163]. Alterations in the visible light absorption of electrochromic fibres lay the foundation for integrating thermal management with camouflage.

Currently, dynamic radiative thermal management technology remains relatively constrained and in its preliminary research stages, given the application requirements for smart textiles such as flexibility, non-toxicity, wash resistance, and cyclic stability. Present approaches predominantly utilise Janus structures for mechanical flipping to achieve switching, alongside dynamically regulating mid-infrared emissivity. This is achieved by controlling the opening and closing of pore channels within fibres or modulating charge carriers in electrically conductive fibres.

Building walls

The application of dynamic radiant thermal management technology in building walls can significantly enhance energy efficiency, improve indoor thermal comfort, and reduce reliance on active heating/cooling systems. Dynamic materials respond to external environmental changes, automatically balancing indoor-outdoor heat exchange to address the traditional wall issue of being 'cold in winter and hot in summer' [164]. Achieving year-round energy savings in buildings is crucial for carbon neutrality and sustainability. This is accomplished by passively dissipating heat into the cold outer space during summer and absorbing heat from the sun's warmth in winter, dynamically regulating internal temperatures [165]. Similar to smart textiles, thermal management technologies for building walls using smart materials primarily rely on dynamically switching between high absorption and high reflection of solar bands, alongside regulating infrared emissivity between the interior and exterior.

By dynamically regulating the visible light band through temperature adaptation, thermal management is achieved when applied to building roofs. Colour-adaptive flexible films utilise thermochromic microcapsules to dynamically switch between high reflectance and high absorptance in solar bands, enabling dynamically switchable thermal management in an energy-neutral manner [166,167]. This is achieved by selecting two distinct components of thermochromic microcapsules and fluorescent dyes, to decouple solar reflectance modulation from colour display [88]. The synergistic interaction of these two coloured components yields the desired controllable solar reflectance without altering the displayed colour. Furthermore, an electrically controlled structure dynamically modulates emissivity based on carrier concentration, combined with thin-film interference effects, to dynamically regulate mid-infrared emissivity. This is applied to building roofs for spatial thermal management. For instance, a multi-layer thin-film ultra-thin electrochromic device has been meticulously engineered as a colourful smart infrared emissivity regulator for all-weather thermal management in buildings. By altering optical bandgap and carrier concentration through Li^+ insertion/extraction, combined with surface plasmon resonance (LSPR) and thin-film interference effects, it achieves mid-infrared emissivity regulation (Figure 5b) [138]. The infrared emissivity of the regulator can be electrically controlled in real-time according to seasonal or temperature variations, enabling switching between cooling and heating modes. Furthermore, an array structure fabricated from tungsten-doped vanadium dioxide automatically switches thermal emissivity from 0.20 at ambient temperatures below 15 °C to 0.90 at temperatures above 30 °C (Figure 5c) [133].

Achieving dynamic control across the entire visible, near-infrared, and mid-infrared spectrum remains challenging. Owing to the simplicity of Janus structures and their suitability for large-scale fabrication, they

hold promise for spatial thermal management in building envelopes. Numerous analogous studies have been reported, such as sandwich-structured fabrics composed of vertically aligned graphene, graphene-coated glass fibre fabric, and polyacrylonitrile nanofibres. These fabrics integrate heating and cooling functions on opposite sides through multi-band, synergistic (covering the solar spectrum and mid-infrared range) and asymmetric optical modulation, constituting Janus structures [168]. These dual-functional fabrics demonstrate exceptional performance and high adaptability to dynamic environments in zero-energy-input temperature regulation [169]. Additionally, through external integration, motorised pulling enables flipping between the two sides [170]. Furthermore, thermally controlled self-curling structures have been designed to switch between upper and lower layers [40]. Beyond conventional Janus structures for architectural thermal management, electro-controlled structures dynamically regulate solar band reflectance and mid-infrared emissivity via carrier concentration modulation, achieving full-spectrum dynamic control. This silicon-based device combines lithium-ion electrochemical reactions with reversible lithiation/delithiation processes to induce phase transitions and dimensional changes in silicon material. This enables dynamic regulation of infrared emissivity, simultaneously providing radiative cooling and solar heating capabilities. It achieves summer radiative cooling and winter thermal insulation while possessing high-capacity electrical energy storage [171].

Thermal control coatings for space applications

Space temperatures fluctuate dramatically (from −100 to 150 °C), necessitating dynamic adjustment of surface emissivity to maintain instruments within a narrower temperature range. This ensures material efficacy and reliability, facilitates normal equipment operation, enhances spacecraft reliability under extreme conditions, and reduces the weight and power consumption of active thermal control systems. Effective thermal management technology is crucial for mitigating adverse effects caused by extreme thermal conditions [172].

Temperature-adaptive solar coatings and temperature-adaptive radiative coatings rely on dynamically regulating mid-infrared emissivity, alongside dynamically switching between high reflectance and high absorptance within the solar spectrum. They represent a novel, lightweight, energy-free temperature regulation method for terrestrial objects exhibiting outstanding thermal performance (Figure 5d) [150]. For instance, Wu *et al*. [173] simulated and demonstrated the significant potential of temperature-adaptive solar coatings and temperature-adaptive radiative coatings as passive thermal management technologies for future space objects. Utilising the principle of metal-insulator phase transitions (electronic structure abrupt changes) to modulate mid-infrared emissivity, such as VO_2 for spacecraft thermal control via particle-based smart metasurfaces. These consist of VO_2 particles on an Au substrate forming a lattice array of hollow spheres [174]. The metasurface, featuring VO_2 particles with a high aspect ratio (~10), exhibits perfect emission across the entire mid-infrared spectrum. The emissivity tunability exceeds 0.63. The fundamental mechanism underlying the metasurface is attributed to the drastic change in electron density during phase transition. Concurrent structural design significantly enhances infrared emissivity in the metallic state while constraining it in the dielectric state, thereby achieving dynamic regulation [175]. Similarly, metasurfaces fabricated from VO_2 enable dynamic emission control [176]. This extends to multilayer VO_2-based structures, such as conventional FP cavity configurations [177]. Considering the impact of extreme space en-

vironments on vanadium dioxide, research has developed VO_2 metasurfaces incorporating functional silicon layers. This eliminates the need for additional protective coatings typically required to shield VO_2 from environmental degradation, thereby enabling responsiveness to ambient temperatures and potential long-term stability [178]. The metasurface achieves passive thermal management by autonomously adjusting its absorption and emission responses across a broad bandwidth spanning visible to mid-IR wavelengths. Furthermore, metal-insulator-semiconductor (MIS) structures were employed, wherein the carrier distribution within the semiconductor layer can be electrically controlled to manipulate the material's emissivity [179].

Beyond the aforementioned application scenarios, which encompass electronic device thermal management and outdoor large-scale instrumentation, current research in non-transparent systems primarily focuses on thermal regulation through modulation of mid-infrared emissivity. Constrained by thermal management energy limitations and operational conditions, switching between high reflectivity and high absorption within the solar spectrum enables cooling and heating functions. This approach elevates the upper energy threshold for thermal management, maximising energy efficiency. However, dynamic radiative thermal management for non-transparent systems still faces challenges, such as applications in extreme environments—particularly space applications—and the need to elevate the energy threshold for dynamic regulation to broaden its regional applicability. Looking ahead, advancements in smart materials like metamaterials and AI-driven coatings will further expand the scope of dynamic radiative thermal management. This technology holds promise as a cornerstone for green energy sectors and high-tech industries.

Transparent system

The distinction between transparent systems and non-transparent systems in dynamic radiant heat management applications primarily lies in the fact that non-transparent systems dynamically switch between high reflectance and high absorptance within the solar spectrum (VIS-NIR), whereas transparent systems dynamically regulate between high transmittance and low transmittance. Consequently, their heat management applications predominantly occur in scenarios requiring transmittance control, such as building windows or vehicle windows. As the primary conduit for thermal exchange between buildings and the external environment, windows hold pivotal significance in green building design. Serving as the principal daylighting component, windows simultaneously represent the weakest link in a building envelope's thermal insulation, resulting in low energy utilisation efficiency. By dynamically regulating transmittance in the solar spectrum and emissivity in the mid-infrared range, they control daylighting and indoor temperatures, thereby reducing energy consumption for cooling and heating [180]. Consequently, extensive research on smart windows has been documented, providing clear insights into control methods and core mechanisms across visible, near-infrared, and mid-infrared bands. Furthermore, studies on smart windows encompass dynamic regulation of solar transmittance across near-infrared, visible-near-infrared, and visible-near-infrared-mid-infrared bands, alongside the intelligent evolution of dynamic response from bimodal to multimodal systems.

Single-band regulation

Near-infrared energy constitutes nearly 50% of sunlight. Moreover, as the frequency of near-infrared light

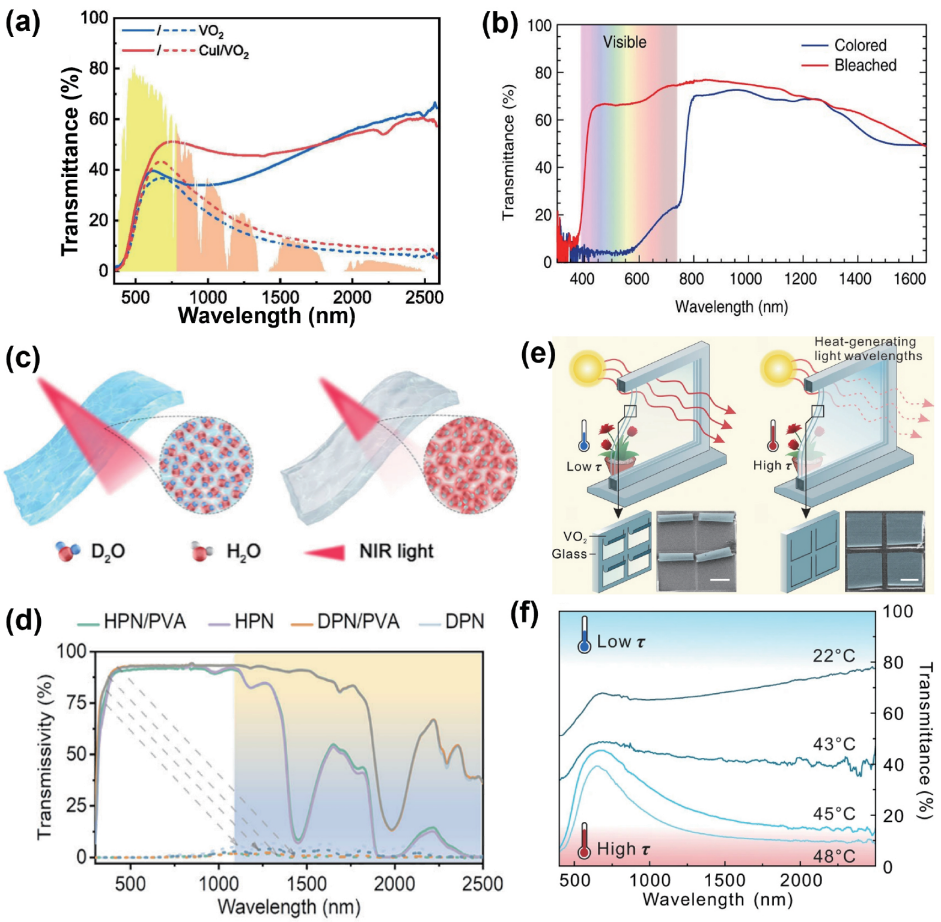

Figure 6 Radiant thermal management application of transparent systems: smart windows. (a) The spectrum of NIR single-wavelength modulated based on vanadium oxide [198]. Copyright©2024, Elsevier. (b) The spectrum of visible light single-wavelength modulation based on perovskite [37]. Copyright©2017, Springer Nature. (c, d) The structure and spectrum of the dual-band modulation based on hydrogels [206]. Copyright©2025, Springer Nature. (e, f) The structure and spectrum of the multimodal dual-band modulation based on vanadium dioxide [207]. Copyright©2022, Springer Nature.

aligns more closely with the resonance frequencies of microscopic particles within materials, it exhibits a stronger thermal effect. Consequently, regulating the transmittance of near-infrared light through dynamically responsive materials can adapt to human living requirements and reduce energy consumption. Classic thermally induced phase-change materials such as niobium oxide and vanadium oxide [181,182] dynamically modulate near-infrared transmittance in response to temperature variations (Figure 6a) [183]. However, niobium oxide's phase transition temperature far exceeds room temperature [184], rendering it unsuitable for smart windows requiring transitions near ambient conditions. Conversely, extensive research exists on vanadium dioxide applications in smart windows, such as inkjet-printed vanadium dioxide powders achieving modulation rates of 15.31% [185] though this modulation performance is achieved at the expense of the film's initial transmittance. Moreover, vanadium dioxide exhibits a phase transition temperature as high as 68 °C. Consequently, balancing phase transition temperature, initial transmittance, and film modulation efficiency remains a pressing challenge in research on vanadium dioxide applications for smart windows [186–188]. Studies have employed doping with elements such as W, [189–191] Mo, [192] Co [193]

to induce lattice distortion while altering the valence state of vanadium, thereby reducing its phase transition temperature while maintaining modulation efficiency [194]. To address vanadium dioxide's susceptibility to degradation, protective layers have been incorporated. For instance, vanadium dioxide powders can be coated with hydrophobic resin films [181] or encapsulated within hybrid inorganic-organic coating structures such as VO_2@MgF_2@PDA [195], enhancing both switching speed and durability. Furthermore, protective layers covering the surface of magnetron-sputtered vanadium dioxide films [196], such as V_2O_3 [182], HfO_2 [197], and CuI [198], enhance cycling stability while maintaining modulation efficiency. Most electrochromic material systems achieve visible-near-infrared co-modulation [199]. However, electrochromic devices are constrained by the transmission characteristics of electrodes such as ITO and FTO in the near-infrared band (where transmission sharply declines beyond 1500 nm), limiting their modulation efficiency due to restricted control wavelengths [200]. Consequently, research into dynamic modulation of electrochromic materials solely within the near-infrared band remains relatively scarce.

The energy proportion within the visible light spectrum reaches as high as 43%, and given the limitations of single-band regulation in the near-infrared region, certain material systems enable dynamic control of transmittance for specific visible light wavelengths [200]. Building upon the electrochromic devices introduced earlier, Yang *et al*. [201] developed an 'electrodes-free' electrochromic (EC) device utilising the reversible deposition of MnO_2 to achieve colour fading and visible light regulation, leveraging its complex multilayer structure. Furthermore, the perovskite material system ABX_3 exhibits crystal structure transformations under temperature control, enabling transparency switching (Figure 6b). However, as its phase transition temperature exceeds 100 °C [202], far surpassing practical application scenarios, subsequent research co-embedded methanol (rather than water) with methylammonium iodide and adjusted the hydrogen-bond chemistry of the reservoir phase to control the transition temperature. This reduced the phase transition temperature to below 30 °C, demonstrating its potential for practical application [203]. Subsequent studies developed small-molecule-responsive perovskite systems [89]. Addressing stability concerns in perovskite-based smart windows, Cao *et al*. [92] designed a multilayer structure inspired by mask architecture, effectively ensuring structural integrity and enhancing device cycling stability. Furthermore, certain liquid crystal systems including polymer-dispersed liquid crystals [81,204] and cholesteric liquid crystals [84,205], effectively modulate visible light via light scattering under electric field control. However, their high drive voltage requirements (at least tens of volts) currently limit their energy-saving potential for smart window applications. Furthermore, certain photochromic systems, such as spiropyran derivatives [100], can effectively modulate visible light. Photoisomerisation induces a colour transition from colourless to coloured states, enabling colour switching. However, for outdoor applications in smart windows, the stability and cycling lifetime of organic molecules remain significant challenges.

Dual-band regulation based on dual-modality and multi-modality

To enhance energy-saving performance, subsequent research focused on dual-mode regulation across the visible-near-infrared spectrum, achieving modulation efficiencies exceeding 30% through control of only high and low temperature modes. For instance, conventional hydrogel systems exhibit visible light transmittance exceeding 90% while maintaining modulation efficiencies surpassing 60%, or even higher. Given these advantages, dual-mode regulation across visible-near-infrared wavelengths in hydrogels has been

extensively investigated. Regarding phase transition temperature, pure PNIPAm exhibits a critical transition temperature of approximately 32 °C. Guo *et al*. [72] modified PNIPAm by employing different solvents to reduce intermolecular forces between PNIPAm and water, as well as water's surface tension, thereby lowering the critical transition temperature to 22–28 °C. Furthermore, by introducing *in situ* radical polymerisation and non-covalent crosslinking in a PNIPAm-water-glycerol binary solvent system, excellent freeze resistance was maintained at −18 °C, enhancing stability [208]. Regarding response speed, one study synthesised a solid-liquid switchable thermochromic hydrogel by crosslinking PNIPAm with 3-aminopropyltriethoxysilane (AMEO) via dynamic imine bonds [209]. However, the water component in hydrogels exhibits strong absorption in the NIR band, limiting modulation efficiency and presenting a significant bottleneck for further performance enhancement. Consequently, Wu *et al*. [206] prepared isotope-driven D_2O-hydrogel thermochromic smart windows by substituting ordinary water with heavy water (D_2O) (Figure 6c). This reduced absorption in the near-infrared band during the initial state (Figure 6d).

To adapt to variable climatic conditions and human requirements, diversified modalities are increasingly crucial. For instance, most single-system electrochromic devices exhibit varying degrees of transmittance reduction in their films under different drive voltages, thereby enabling regulation of multiple states [201,210]. For example, Cao *et al*. [211] employed Na^+ pumps to expel H^+, achieving ultrafast all-solid-state WO_3 electrochromic colouration. However, this state proves unstable; under sustained low voltage for sufficiently prolonged periods, the colouration process persists. Consequently, it does not strictly qualify as multimodal. Similarly, in photochromic WO_3 systems, the degree of colouration varies with light intensity and exposure duration [54]. Thus, researchers have initiated a series of studies on multimodal regulation for smart windows. For instance, the dual-mode regulation of classic vanadium dioxide and its modulation rate in the NIR band have approached their thresholds, making further breakthroughs challenging. Inspired by blinds, Mei and Cao *et al*. [207] employed self-curling technology to detach strain-induced vanadium dioxide films from glass substrates and curl them into 'slat' arrays for smart windows (Figure 6e and f). However, in devices combining $Nb_{18}W_{16}O_{93}$ and Prussian blue (PB) as complementary electrochromic layers, the co-intercalation of cations and anions through charge-balancing design enables diverse colour and spectral modulation alongside stable multimodal control capabilities [212]. Beyond single-system regulation, studies indicate that multi-system combinations can overcome limitations in modulation rates and multi-modality. For instance, co-assembly of photoswitchable organic crosslinkers (Azo-Ch) and superparamagnetic inorganic nanoparticles (Fe_3O_4@SiO_2) yields organic-inorganic semi-interpenetrating network composite gels, enabling orthogonal control via light and magnetic fields [94]. Furthermore, combining electrochromic $W_{18}O_{49}$ with thermochromic W-VO_2 nanowires effectively enhances sunlight modulation and thermal management capabilities in smart windows [213]. Additionally, multifunctional smart windows integrating light-responsive tungsten oxide particles with thermochromic hydrogels [214], and photo-electro dual-responsive films combining WO_3, ethylene glycol (EG), and Ag, enabling simultaneous photochromic and electrochromic functionality [215], achieve visible-to-near-infrared multimodal regulation through combined response mechanisms.

Furthermore, subsequent research on smart windows has demonstrated multi-modal control by separately regulating the visible-near-infrared spectrum. This is achieved through a '1+1' combination of material systems with identical response mechanisms, enabling multi-modal band-specific regulation of visible and near-infrared light. For instance, Cao *et al*. [46] employed thermochromic paraffin wax and vanadium

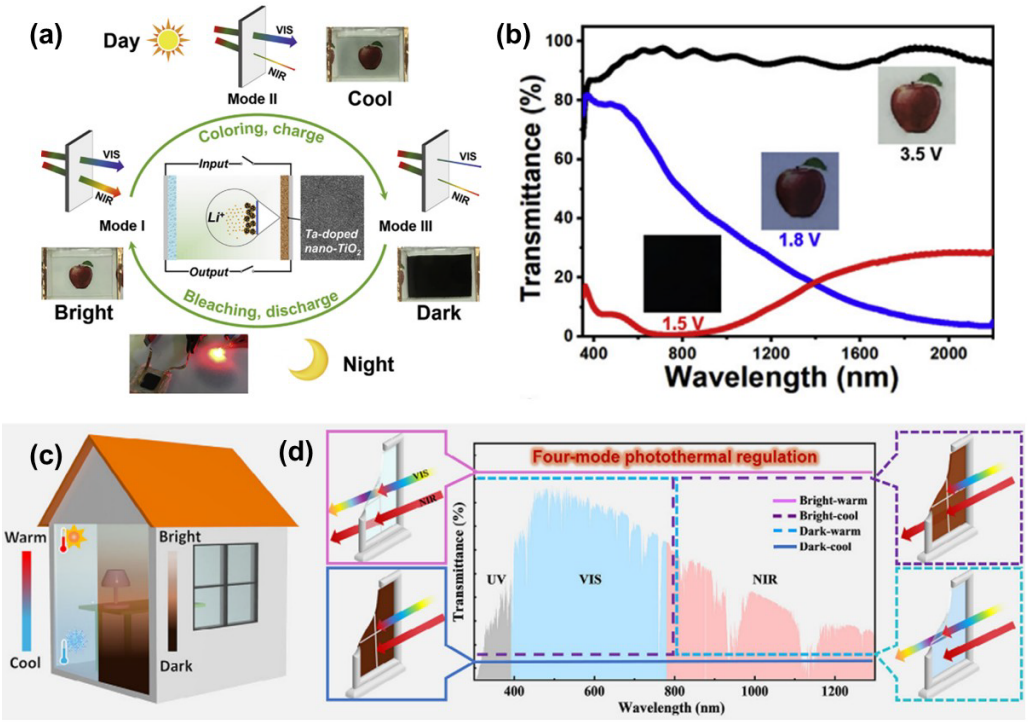

Figure 7 (a, b) The electrochromic structure and spectrum for multimodal dual-band modulation [216]. Copyright©2019, Elsevier. (c, d) Ideal spectra that can be independently controlled in the near-infrared band [218]. Copyright©2025, John Wiley and Sons.

dioxide, utilising the optical scattering transition between paraffin and the substrate to regulate visible light, while vanadium dioxide controlled the near-infrared spectrum. This approach prioritised near-infrared regulation, balancing energy efficiency and visibility in smart window applications. However, its visible light regulation relies on optical scattering, thereby introducing haze issues. Conversely, Lee *et al*. [216] proposed a dual-frequency electrochromic device employing composition-optimised Ta-doped TiO_2 nanocrystals as multifunctional active material. This enables simultaneous provision of high charge storage capacity, high bistability, and long-lifetime electrochromic behaviour across three distinct operating modes: (1) VIS and NIR transparent 'bright' mode; (2) VIS transparent and NIR opaque 'cool' mode; (3) fully opaque 'dark' mode (Figure 7a and b). Similarly, Long *et al*. [217] employed Nb-doped anatase TiO_2 nanocrystals, whose products lack organic ligands, thereby reducing near-infrared absorption. This enables preferential near-infrared control below 1600 nm, achieving multi-modal regulation. Moreover, its visible-light regulation operates by enhancing light absorption to reduce transmittance, thereby mitigating haze issues. Cai *et al*. [218] employed a mixed electrolyte to decouple reversible deposition and ion adsorption in WO_3/MnO_2-based smart windows, achieving independent and efficient VIS-NIR regulation (Figure 7c and d). Cu^{2+}/Mn^{2+} ions in the hybrid electrolyte enhance proton adsorption on the WO_3 surface while inhibiting proton insertion, thereby providing state-of-the-art near-infrared modulation for WO_3 electrodes. The synergistic interaction between protons and Cu^{2+}/Mn^{2+} ions promotes reversible MnO_2 electrodeposition on the electrode, triggering independent VIS light tuning. Li *et al*. [43] proposed dual-operating-mode electrochromism through integrating complementary $Ce_4W_9O_{33}$/NiO devices with Zn anode-based electrochromic

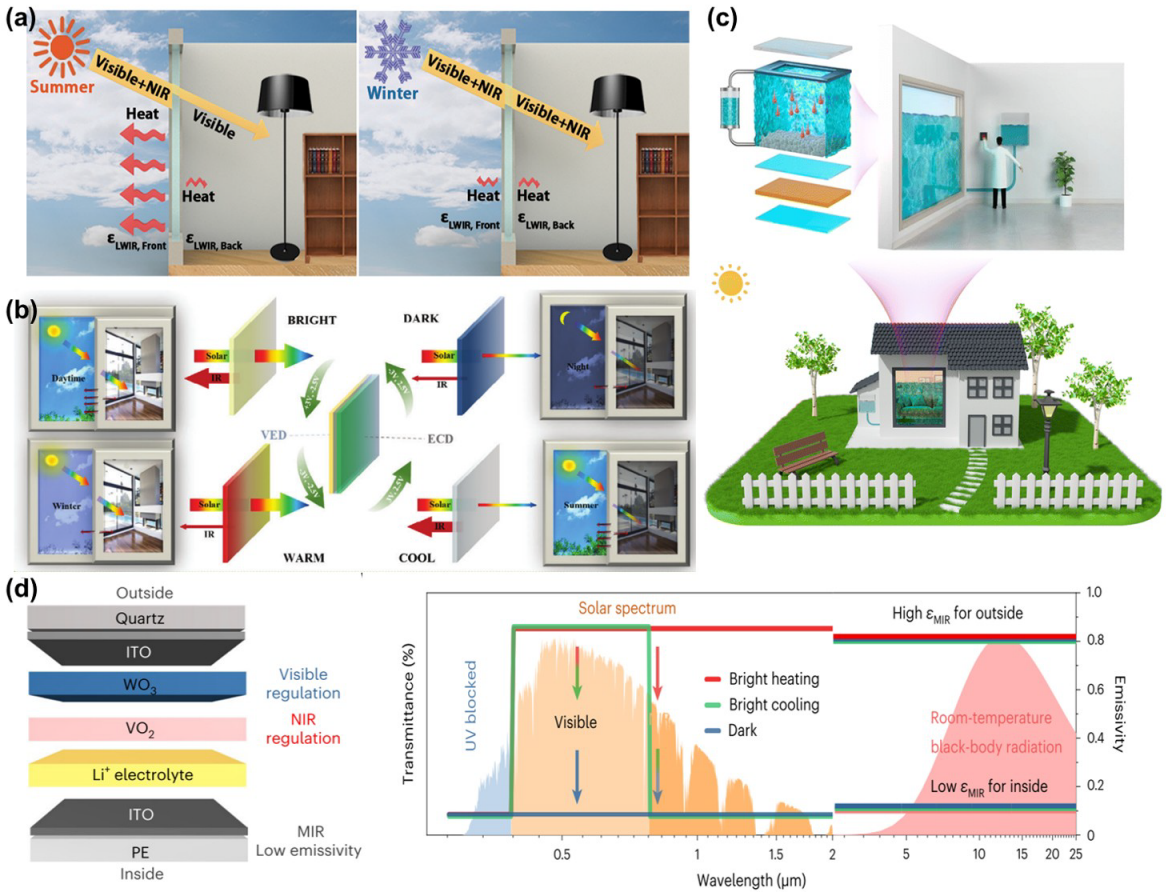

Figure 8 (a) Dual-modal modulation of the VIS-NIR-MIR three-band system [219]. Copyright©2021, The American Association for the Advancement of Science. (b) Multi-band dynamic regulation where the solar band emission rate and infrared emission rate are independent of each other [221]. Copyright©2023, John Wiley and Sons. (c) Independent regulation of infrared emissivity for multi-band three-modal modulation [38]. Copyright©2025, Royal Society of Chemistry. (d) Multi-band dynamic regulation where the solar band emission rate and infrared emission rate are independent of each other [222]. Copyright©2024, Springer Nature.

devices ($Ce_4W_9O_{33}$/Zn/NiO devices), enabling multimodal band-selective regulation of visible and near-infrared light. Research on visible-near-infrared multimodal band-selective control primarily focuses on achieving near-infrared priority control (three modes) and independent visible-near-infrared control (four modes). Regarding visible light control, the underlying principle shifts from light scattering to light absorption, necessitating application-specific determination. For privacy protection applications, light scattering offers greater advantages; conversely, when enhancing energy efficiency while maintaining visibility is required, light absorption-based control becomes more compelling.

Tri-band regulation based on multimodal approaches

With the advancement of radiative cooling technology, thermal radiation regulation in the mid-infrared spectrum is increasingly being integrated into smart window systems. Under ideal conditions, during periods of high ambient temperatures, it is desirable for the sky-facing exterior surface of the smart window to maintain high emissivity. This facilitates thermal radiation exchange between the window and the ideal

cooling source of outer space, thereby enhancing the cooling effect. Conversely, during cold weather, the smart window should maintain low emissivity to minimise heat exchange. Consequently, building upon research into dual-band dynamic regulation across the visible-near-infrared spectrum, achieving tri-band dynamic control across visible light, near-infrared, and mid-infrared has emerged as a key research focus to further enhance energy-saving performance. Long *et al*. [219] pioneered this field by proposing the use of VO_2 as a switch for dynamically regulating emissivity within a Fabry-Perot (F-P) cavity, thereby initiating tri-band regulation research in smart windows (Figure 8a). For instance, Yang *et al*. [220] combined polymeric dispersed liquid crystals with high mid-infrared emissivity and low-emissivity hydrogel PNIPAm. They achieved multi-band regulation of visible light, near-infrared, and long-wave infrared radiation by seasonally reversing mid-infrared control and employing electrothermal dual-control regulation of the solar band (VIS-NIR). Notably, alterations in mid-infrared emissivity occur independently of solar band regulation. This Janus-like structure's reversal modifies emissivity, differing fundamentally from dynamic control mechanisms. Conversely, Huang *et al*. [44] exploited temperature-triggered water capture and release induced by PNIPAm phase transitions to achieve simultaneous solar band and emissivity regulation, thereby realising dual-mode tri-band control.

To achieve multimodal regulation, the mid-infrared spectrum is first decoupled from solar band control. For instance, a dual-response mechanism employs a paper-cut structure of flexible thermochromic materials, with a surface layer coated in low-emissivity silver nanowires. This configuration enables temperature-controlled response to solar radiation while mechanically stretchable emission regulation [62]. Furthermore, independent mid-infrared regulation is achieved by integrating an all-solid-state transparent emissivity modulator with a solar band control device (Figure 8b). For instance, Li *et al*. [221] integrated an all-solid-state transparent variable infrared emissivity device (ITO/SiO_2/ITO, VED) with a WO_3 electrochromic device. Under dual independent power sources, this configuration separately controls mid-infrared emissivity and solar band transmittance. The top and bottom ITO layers form two mirrors, with the intermediate SiO_2 layer acting as a resonant cavity. Infrared light of specific wavelengths undergoes multiple reflections within the cavity, creating resonance-enhanced absorption. By applying positive/negative bias to alter the carrier concentration in the top ITO layer, the mid-infrared emission is modulated based on the principle of carrier concentration modulation. These adjustment methods resemble a '1+1' combination approach, operating independently yet resulting in cumbersome device structures and complex fabrication. Consequently, coupling mid-infrared emissivity regulation with visible-near-infrared dynamic control presents a significant challenge. Zhang *et al*. [38] achieved complete switching of MIR emissivity between 0.19 and 0.93 by toggling the presence/absence of an electrolyte. Crucially, while maintaining high emissivity with the electrolyte present, they simultaneously realised dynamic control of visible-near-infrared transmittance, effectively leveraging the coupled relationship for synergistic regulation (Figure 8c). Furthermore, in tri-band dynamic regulation, multimodal control optimising full-spectrum (visible, near-infrared, mid-infrared) photothermal exchange is particularly crucial for smart window development. Consequently, Cao *et al*. [222] employed Li^+ ions to diffuse into the monoclinic VO_2 and WO_3 layers under distinct applied voltages, inducing phase transitions to tetragonal Li_xVO_2 and cubic Li_yWO_3. This approach enables multimodal regulation across both the near-infrared band and the visible-near-infrared dual-band spectrum (Figure 8d). Concurrently, by integrating high- and low-emissivity layers on the upper and lower surfaces respectively, emissivity control is decoupled from the solar spectrum, enabling tri-band multimodal regulation.

SUMMARY AND OUTLOOK

Smart windows not only provide users with more comfortable living and working environments but also reduce energy consumption and carbon emissions, making significant contributions to global sustainable development goals. To maximise energy utilisation, band modulation in smart windows applied within transparent systems has evolved from single-band to dual-band and subsequently to triple-band modulation. Therefore, the future development of smart windows towards full-band modulation is undoubtedly imminent. Whether a hierarchical relationship exists among the three bands or whether independent control of all three bands should be pursued remains a matter worthy of consideration. We contend that regulating the optical behaviour within the visible spectrum is particularly crucial, with the two dominant phenomena of light scattering and light absorption requiring consideration in specific application scenarios. Consequently, under the premise of achieving full-spectrum dynamic regulation, multi-modal control of visible light may represent a future developmental trajectory. At the current research stage, near-infrared prioritisation and independent mid-infrared control have been achieved. However, visible light regulation still faces several challenges, including determining the optimal light control method, achieving synergistic regulation with near-infrared and mid-to-far-infrared light, and balancing visibility with energy efficiency. Thus, the development of smart windows necessitates prioritisation in VIS-NIR-MIR control, making independent regulation across all three bands an urgent research priority.

Considering the intrinsic properties of smart windows, such as daylighting, visual comfort, and visibility, the independent regulation of visible light becomes increasingly crucial. Moreover, the separate control of NIR and MIR enables stepwise modulation of energy, rendering VIS-NIR-MIR independent regulation of paramount significance for the advancement of smart windows. Simultaneously, research into independent control expands application possibilities in other domains, such as outdoor visible-infrared dual-band camouflage. Based on different dimming methods, the transmittance of visible and near-infrared bands can be dynamically regulated. Within the visible spectrum, transmittance is regulated through scattering and reflection to influence visibility. Future approaches will thus focus on dynamically controlling visible light transmittance via absorption. Furthermore, absorption-based regulation enables integration with other devices, such as solar absorbers and photovoltaic cells to maximise energy utilisation.

Funding

This work was supported by the National Key Research and Development Program of China (2021YFA0718900), the National Natural Science Foundation of China (62175248, 62575296 and U24A2061), and the Shanghai Science and Technology Funds (23ZR1481900 and 25ZR1401373).

Conflict of interest

The authors declare no conflict of interest.

References

1 Lesk C, Rowhani P, Ramankutty N. Influence of extreme weather disasters on global crop production. *Nature* 2016; **529**: 84–87.

2 Le Quéré C, Andrew RM, Friedlingstein P, *et al.* Global carbon budget 2018. *Earth Syst Sci Data* 2018; **10**: 2141–

2194.
3 Easterling DR, Meehl GA, Parmesan C, *et al.* Climate extremes: Observations, modeling, and impacts. *Science* 2000; **289**: 2068–2074.
4 Lee M, Kim G, Jung Y, *et al.* Photonic structures in radiative cooling. *Light Sci Appl* 2023; **12**: 134.
5 Fan S, Li W. Photonics and thermodynamics concepts in radiative cooling. *Nat Photon* 2022; **16**: 182–190.
6 Liang J, Wu J, Guo J, *et al.* Radiative cooling for passive thermal management towards sustainable carbon neutrality. *Natl Sci Rev* 2023; **10**: nwac208.
7 Lu G, Du F, Wang Z, *et al.* Scalable metasurface-enhanced supercool cement. *Sci Adv* 2025; **11**: eadv2820.
8 Lu G, She W, Tong X, *et al.* Radiative cooling potential of cementitious composites: Physical and chemical origins. *Cement Concrete Compos* 2021; **119**: 104004.
9 Nie H, Huang L, Xu X, *et al.* High performance radiative cooling coating with dense surface structure via closed-cell microstructures and uniformly dispersed scatterers. *Small* 2025; **21**: 2507594.
10 Meng X, Chen Z, Qian C, *et al.* Durable and mechanically robust superhydrophobic radiative cooling coating. *Chem Eng J* 2023; **478**: 147341.
11 Hu X, Tao G, Zhou H, *et al.* Biaxial stretching unlocks durable, high-performance radiative cooling. *Matter* 2025; **8**: 102321.
12 Zeng S, Pian S, Su M, *et al.* Hierarchical-morphology metafabric for scalable passive daytime radiative cooling. *Science* 2021; **373**: 692–696.
13 Mousavi SAA, Aghakhani H, Baghapour B, *et al.* Integrating radiative cooling and thermoelectric: A comprehensive review. *Renew Sustain Energy Rev* 2025; **222**: 115946.
14 Ishii S, Bourgès C, Tanjaya NK, *et al.* Transparent thermoelectric device for simultaneously harvesting radiative cooling and solar heating. *Mater Today* 2024; **75**: 20–26.
15 Lee KW, Yi J, Kim MK, *et al.* Transparent radiative cooling cover window for flexible and foldable electronic displays. *Nat Commun* 2024; **15**: 4443.
16 Yang R, Niu D, Pu JH, *et al.* Passive all-day freshwater harvesting through a transparent radiative cooling film. *Appl Energy* 2022; **325**: 119801.
17 Jin Y, Jeong Y, Yu K. Infrared-reflective transparent hyperbolic metamaterials for use in radiative cooling windows. *Adv Funct Mater* 2023; **33**: 2207940.
18 Zhai Y, Ma Y, David SN, *et al.* Scalable-manufactured randomized glass-polymer hybrid metamaterial for daytime radiative cooling. *Science* 2017; **355**: 1062–1066.
19 Xu J, Huo X, Yan T, *et al.* All-in-one hybrid atmospheric water harvesting for all-day water production by natural sunlight and radiative cooling. *Energy Environ Sci* 2024; **17**: 4988–5001.
20 Li T, Wu M, Xu J, *et al.* Simultaneous atmospheric water production and 24-hour power generation enabled by moisture-induced energy harvesting. *Nat Commun* 2022; **13**: 6771.
21 Wang S, Wu M, Han H, *et al.* Regulating cold energy from the universe by bifunctional phase change materials for sustainable cooling. *Adv Energy Mater* 2024; **14**: 2402667.
22 Wang Z, Kim SK, Hu R. Self-switchable radiative cooling. *Matter* 2022; **5**: 780–782.
23 Agbo EP, Nkajoe U, Okono MA, *et al.* Temperature and solar radiation interactions in all six zones of Nigeria. *Ind J Phys* 2023; **97**: 655–669.
24 Li J, Cui X, Yang J. Multi-scale correlation analysis between geometric parameters and solar radiation in high density urban environment——Case study in Nanjing. *Front Architectural Res* 2025; **14**: 248–266.
25 Song J, Jeong KJ, Baik G, *et al.* Air-gap controlled smart window for spectral and angular selective modulation of solar radiation. *Energy Convers Manage* 2025; **324**: 119237.
26 Zhou Z, Fang Y, Wang X, *et al.* Synergistic modulation of solar and thermal radiation in dynamic energy-efficient windows. *Nano Energy* 2022; **93**: 106865.
27 Wei D, Wang C, Shi G, *et al.* Enabling self-adaptive water-energy-balance of photothermal water diode evaporator:

Dynamically maximizing energy utilization under the ever-changing sunlight. *Adv Mater* 2024; **36**: 2309507.

28 Jo HJ, Jang YJ, Kim HD, *et al.* Glare-free, energy-efficient smart windows: A pedestrian-friendly system with dynamically tunable light and heat regulation. *ACS Energy Lett* 2025; **10**: 2997–3004.

29 Li D, Kou E, Li W, *et al.* Oxidation-induced quenching mechanism of ultrabright red carbon dots and application in antioxidant RCDs/PVA film. *Chem Eng J* 2021; **425**: 131653.

30 Ghosh S, Smalyukh I. Electrical switching of nematic plasmonic nanocolloids for infrared solar gain control (advanced optical materials 20/2022). *Adv Opt Mater* 2022; **10**: 2270079.

31 Chen Q, Huang X, Lu Y, *et al.* Mechanically tunable transmittance convection shield for dynamic radiative cooling. *ACS Appl Mater Interfaces* 2024; **16**: 21807–21817.

32 Wang J, Tan G, Yang R, *et al.* Materials, structures, and devices for dynamic radiative cooling. *Cell Rep Phys Sci* 2022; **3**: 101198.

33 Zhao B, Xuan Q, Xu C, *et al.* Considerations of passive radiative cooling. *Renew Energy* 2023; **219**: 119486.

34 Liu S, Chen G, Li J, *et al.* Smart skin for zero energy buildings: A review of thermoresponsive spectral-adaptive envelopes. *Adv Mater* 2025; **8**: e11392.

35 Xie L, Wang X, Bai Y, *et al.* Fast-developing dynamic radiative thermal management: Full-scale fundamentals, switching methods, applications, and challenges. *Nano-Micro Lett* 2025; **17**: 146.

36 Xu T, Yeow Seow JZ, Tan S, *et al.* Radiative smart fibers and textiles: Thermal management and beyond. *ACS Nano* 2025; **19**: 32995–33007.

37 Wheeler LM, Moore DT, Ihly R, *et al.* Switchable photovoltaic windows enabled by reversible photothermal complex dissociation from methylammonium lead iodide. *Nat Commun* 2017; **8**: 1722.

38 Huang Y, Wu S, Zhao S, *et al.* A novel liquid flow electrochromic smart window for all-year-round dynamic photothermal regulation. *Energy Environ Sci* 2025; **18**: 1824–1834.

39 Zhang XA, Yu S, Xu B, *et al.* Dynamic gating of infrared radiation in a textile. *Science* 2019; **363**: 619–623.

40 Zhang Q, Lv Y, Wang Y, *et al.* Temperature-dependent dual-mode thermal management device with net zero energy for year-round energy saving. *Nat Commun* 2022; **13**: 4874.

41 Chen S, Jiang G, Zhou J, *et al.* Robust solvatochromic gels for self-defensive smart windows. *Adv Funct Mater* 2023; **33**: 2214382.

42 Zhang R, Song Z, Cao W, *et al.* Multispectral smart window: Dynamic light modulation and electromagnetic microwave shielding. *Light Sci Appl* 2024; **13**: 223.

43 Ma D, Yang T, Feng X, *et al.* Quadruple control electrochromic devices utilizing $Ce_4W_9O_{33}$ electrodes for visible and near-infrared transmission intelligent modulation. *Adv Sci* 2024; **11**: 2307223.

44 Lin C, Hur J, Chao CYH, *et al.* All-weather thermochromic windows for synchronous solar and thermal radiation regulation. *Sci Adv* 2022; **8**: eabn7359.

45 Guo J, Jia H, Jin P, *et al.* Transparent-to-reflective multicolor all-solid-state electrochromic devices for next-generation intelligent display windows. *Adv Mater* 2025; **37**: e00350.

46 Jiao Y, Li Z, Li C, *et al.* Flexible tri-state-regulated thermochromic smart window based on $W_xV_{1-x}O_2$/paraffin/PVA composite film. *Chem Eng J* 2024; **497**: 154578.

47 Lin HC, Zhang MS, Chuang WC. Liquid crystal smart window with bistable and dynamic modes. *J Mol Liquids* 2023; **390**: 123183.

48 Wang L, Li D, Wang Z, *et al.* Indoor dynamic light/thermal environment of smart windows using ATO nanofluids in summer: An experimental study. *Renew Energy* 2024; **234**: 121210.

49 An Y, Fu Y, Dai JG, *et al.* Switchable radiative cooling technologies for smart thermal management. *Cell Rep Phys Sci* 2022; **3**: 101098.

50 Cannavale A, Carlucci F, Pugliese M, *et al.* Low-cost gel-polymer electrolytes for smart windows: Effects on yearly energy consumption and visual comfort. *Energy Build* 2023; **301**: 113705.

51 Tong SW, Goh WP, Huang X, *et al.* A review of transparent-reflective switchable glass technologies for building

facades. *Renew Sustain Energy Rev* 2021; **152**: 111615.

52 Huang NN, Gao J, Sheng SZ, *et al.* Structural design of intelligent reversible two-way structural color films. *Nano Lett* 2023; **23**: 7389–7396.

53 Lee SH, Kang BS, Kwak MK. Magneto-responsive actuating surfaces with controlled wettability and optical transmittance. *ACS Appl Mater Interfaces* 2022; **14**: 14721–14728.

54 Meng W, Kragt AJJ, Gao Y, *et al.* Scalable photochromic film for solar heat and daylight management. *Adv Mater* 2024; **36**: 2304910.

55 Shi K, Liu Z, Yang C, *et al.* Novel biocompatible thermoresponsive poly(*N*-vinyl caprolactam)/clay nanocomposite hydrogels with macroporous structure and improved mechanical characteristics. *ACS Appl Mater Interfaces* 2017; **9**: 21979–21990.

56 Lin G, Chandrasekaran P, Lv C, *et al.* Self-similar hierarchical wrinkles as a potential multifunctional smart window with simultaneously tunable transparency, structural color, and droplet transport. *ACS Appl Mater Interfaces* 2017; **9**: 26510–26517.

57 Xu A, Jiang X, Zhang Z, *et al.* The flexible electronic reflection smart windows for automobiles and architecture. *ACS Appl Mater Interfaces* 2025; **17**: 34193–34205.

58 Ji Z, Gao Z, Zhang T, *et al.* Highly reflective porous SiC with layered nanostructures formed by electrochemical etching. *Appl Surf Sci* 2025; **694**: 162797.

59 Cho SM, Kim S, Kim Y, *et al.* Switchable holographic device based on reversible electrodeposition. *Adv Mater Technologies* 2019; **4**: 1800478.

60 Zhao X, Chen Q, Fan F, *et al.* Dual-band electrochromic smart window for dynamic switching between radiative cooling and solar heating. *Adv Sci* 2025; **12**: e04483.

61 Liang L, Yu R, Ong SJH, *et al.* An adaptive multispectral mechano-optical system for multipurpose applications. *ACS Nano* 2023; **17**: 12409–12421.

62 Wang S, Dong Y, Li Y, *et al.* A solar/radiative cooling dual-regulation smart window based on shape-morphing kirigami structures. *Mater Horiz* 2023; **10**: 4243–4250.

63 Ma H, Tan Y, Cao J, *et al.* Eccentric 1-D magnetic core-shell photonic crystal balls: Ingenious fabrication and distinctive optical properties. *J Mater Chem C* 2018; **6**: 4531–4540.

64 Loiko VA, Berdnik VV. Radiative transfer in a layer of oriented spheroidal particles with oblique incidence of light. *Part Part Syst Charact* 1998; **15**: 115–121.

65 Ji S, Woo HJ, Lee SG, *et al.* Advancing nano-optical investigations: Metallic and dielectric mie particles in SPM techniques and their emerging applications. *Appl Phys Rev* 2025; **12**: 031316.

66 Li J, Lu X, Zhang Y, *et al.* Dynamic refractive index-matching for adaptive thermoresponsive smart windows. *Small* 2022; **18**: 2201322.

67 Yoon W, Lim S, Rim M, *et al.* Photo- and thermo-responsive switchable smart windows developed by the control of 3D molecular orientation of chiral liquid crystals with azobenzene molecular engineering. *Adv Funct Mater* 2025; **35**: 2425115.

68 Chen C, Yao H, Chen Y, *et al.* Ultradurable omni-liquid-repellent smart window as a high-performance wettability/transparency manipulator enabled via laser-writing magnetism-actuated microshutters. *Adv Funct Mater* 2023; **33**: 2308314.

69 Otaegui JR, Ruiz-Molina D, Hernando J, *et al.* Multistimuli-responsive smart windows based on paraffin-polymer composites. *Chem Eng J* 2023; **463**: 142390.

70 Li B, Xu F, Guan T, *et al.* Self-adhesive self-healing thermochromic ionogels for smart windows with excellent environmental and mechanical stability, solar modulation, and antifogging capabilities. *Adv Mater* 2023; **35**: 2211456.

71 Zhao C, Liu G, Lin Y, *et al.* Diphylleia grayi-inspired intelligent temperature-responsive transparent nanofiber membranes. *Nano-Micro Lett* 2024; **16**: 65.

72 Ding Y, Duan Y, Yang F, *et al.* High-transmittance pNIPAm gel smart windows with lower response temperature and

stronger solar regulation. *Chem Eng J* 2023; **460**: 141572.

73 Yu Z, Ma Y, Mao L, *et al.* Bidirectional optical response hydrogel with adjustable human comfort temperature for smart windows. *Mater Horiz* 2024; **11**: 207–216.

74 Chen B, Feng Q, Liu W, *et al.* Review on mechanoresponsive smart windows: Structures and driving modes. *Materials* 2023; **16**: 779.

75 Kim H, Ge D, Lee E, *et al.* Multistate and on-demand smart windows. *Adv Mater* 2018; **30**: 1803847.

76 Zhao F, Wang M, Huang Z, *et al.* Bio-inspired mechanically responsive smart windows for visible and near-infrared multiwavelength spectral modulation. *Adv Mater* 2024; **36**: 2408192.

77 Zhan H, Cheng W, Liu F, *et al.* Resilient and robust mechanoresponsive polydimethylsiloxane/SiO_2 composites induced by interfacial enhancement. *J Colloid Interface Sci* 2025; **690**: 137361.

78 Zhu S, Liu Y, Guo W, *et al.* Humidity-driven dynamic based on polystyrene-contained gelatin (Gel-PS) and PDMS bilayer wrinkling system. *Adv Funct Mater* 2023; **33**: 2301850.

79 Guo J, Wu S, Wang Y, *et al.* A salt-triggered multifunctional smart window derived from a dynamic polyampholyte hydrogel. *Mater Horiz* 2022; **9**: 3039–3047.

80 Liu C, Yang L, Sun Y, *et al.* Hydrogel-coated polydimethylsiloxane with reversible transparency for advanced optical switching. *ACS Nano* 2025; **19**: 9017–9028.

81 Qin J, Yuan B, Yang Y, *et al.* A spectrum-tailored polymer dispersed liquid crystal film for energy-saving smart windows. *Small* 2025; **21**: 2409347.

82 Wang J, Meng C, Wang CT, *et al.* A fully self-powered, ultra-stable cholesteric smart window triggered by instantaneous mechanical stimuli. *Nano Energy* 2021; **85**: 105976.

83 Li B, Valenzuela C, Liu Y, *et al.* Free-standing bacterial cellulose-templated radiative cooling liquid crystal films with self-adaptive solar transmittance modulation. *Adv Funct Mater* 2024; **34**: 2402124.

84 Liu H, Guo ZH, Xu F, *et al.* Triboelectric-optical responsive cholesteric liquid crystals for self-powered smart window, E-paper display and optical switch. *Sci Bull* 2021; **66**: 1986–1993.

85 Zhang H, Liu QC, Zhou CQ, *et al.* Photocatalytic applications of 2D surface decorated boron phosphides: A density functional theory investigation. *Appl Surf Sci* 2022; **592**: 153236.

86 Rhatigan S, Nolan M. Impact of surface hydroxylation in MgO-/SnO-nanocluster modified TiO_2 anatase (101) composites on visible light absorption, charge separation and reducibility. *Chin Chem Lett* 2018; **29**: 757–764.

87 Tan C, Sun D, Xu D, *et al.* Tuning electronic structure and optical properties of ZnO monolayer by Cd doping. *Ceramics Int* 2016; **42**: 10997–11002.

88 Yin Y, Sun P, Zeng Y, *et al.* A colored temperature-adaptive cloak for year-round building energy saving. *Adv Energy Mater* 2024; **14**: 2402202.

89 He H, Liu S, Du Y, *et al.* Enhancing stability: Two-dimensional thermochromic perovskite for smart windows in building applications. *Adv Funct Mater* 2024; 2417582.

90 Zhang R, Liu S, An Y, *et al.* Ultra low-haze and high transparency thermochromic perovskite smart windows with high solar modulation ability. *Nano Energy* 2025; **139**: 110978.

91 Zhang Y, Wang Z, Hu S, *et al.* Robust and swiftly reversible thermochromic behavior of a 2D perovskite of $(C_6H_4(CH_2NH_3)_2)(CH_3NH_3)[Pb_2\ I_7]$ for smart window and photovoltaic smart window applications. *ACS Appl Mater Interfaces* 2021; **13**: 12042–12048.

92 Liu S, Li Y, Wang Y, *et al.* Mask-inspired moisture-transmitting and durable thermochromic perovskite smart windows. *Nat Commun* 2024; **15**: 876.

93 Jin J, Zhang J, Zhang J, *et al.* Minute-level room-temperature switching and long cycle stability of thermochromic inorganic perovskite smart windows. *Adv Mater* 2025; **37**: 2416146.

94 Wang M, Nie C, Liu J, *et al.* Organic-inorganic semi-interpenetrating networks with orthogonal light- and magnetic-responsiveness for smart photonic gels. *Nat Commun* 2023; **14**: 1000.

95 Kang M, Deng Y, Oderinde O, *et al.* Sunlight-driven photochromic hydrogel based on silver bromide with antibacterial

property and non-cytotoxicity. *Chem Eng J* 2019; **375**: 121994.

96 Jiao X, Liu Y, Zhao X. Advancements in TiO_2-based multi-composite photochromic materials: A review. *J Industrial Eng Chem* 2025; **146**: 109–121.

97 Eglītis R, Šutka A. Photochromic TiO_2/PEGDA organogels. *Photochem Photobiol Sci* 2022; **21**: 545–555.

98 Cheng X, Zhang B, Lei G, *et al.* Solar-tunable reversible photochromic smart window based on BiOCl/CA hydrogel. *Adv Opt Mater* 2025; **13**: 01228.

99 Zou J, Liao J, He Y, *et al.* Recent development of photochromic polymer systems: Mechanism, materials, and applications. *Research* 2024; **7**: 0392.

100 Wang L, Liu Y, Zhan X, *et al.* Photochromic transparent wood for photo-switchable smart window applications. *J Mater Chem C* 2019; **7**: 8649–8654.

101 Ube T, Yoshida M, Kurihara S, *et al.* Sunlight-driven smart windows with a wide temperature range of optical switching based on chiral nematic liquid crystals. *ACS Appl Mater Interfaces* 2024; **16**: 28638–28644.

102 Fan S, Lam Y, Yang J, *et al.* Development of photochromic poly(azobenzene)/PVDF fibers by wet spinning for intelligent textile engineering. *Surfs Interfaces* 2022; **34**: 102383.

103 Xie Z, Liu Q, Zhang Q, *et al.* Fast-switching quasi-solid state electrochromic full device based on mesoporous WO_3 and NiO thin films. *Sol Energy Mater Sol Cells* 2019; **200**: 110017.

104 Guo X, Chen J, Eh ALS, *et al.* Heat-insulating black electrochromic device enabled by reversible nickel-copper electrodeposition. *ACS Appl Mater Interfaces* 2022; **14**: 20237–20246.

105 Huang B, Wang B, Zhao F, *et al.* Constructing reversible Zn/MnO_2 dual-electrodeposition-based smart window with wide modulation range by an iodide mediator in near-neutral electrolyte. *Adv Opt Mater* 2025; **13**: e01467.

106 Wang J, Zhou Y, Lv Y, *et al.* A reversible MnO_2 deposition-enabled multicolor electrochromic device with efficient tunability of ultraviolet-visible light. *Small* 2024; **20**: 2310229.

107 Wang Q, Cao S, Meng Q, *et al.* Robust and stable dual-band electrochromic smart window with multicolor tunability. *Mater Horiz* 2023; **10**: 960–966.

108 Chiu SH, Widjajana MS, Nor-Azman NA, *et al.* Electrochromic PEDOT: PSS with embedded liquid gallium nanoparticles. *ACS Appl Mater Interfaces* 2025; **17**: 43968–43978.

109 Qiu M, Zhou F, Sun P, *et al.* Unveiling the electrochromic mechanism of Prussian Blue by electronic transition analysis. *Nano Energy* 2020; **78**: 105148.

110 Qian C, Wang P, Guo X, *et al.* High-contrast energy-efficient flexible electrochromic devices based on viologen derivatives and their application in smart windows and electrochromic displayers. *Sol Energy Mater Sol Cells* 2024; **266**: 112669.

111 Li D, Zhou C, Meng Y, *et al.* Deformable thermo-responsive smart windows based on a shape memory polymer for adaptive solar modulations. *ACS Appl Mater Interfaces* 2021; **13**: 61196–61204.

112 Chen C, Yao H, Guo S, *et al.* Ultra-robust joule-heated superhydrophobic smart window: Dually-switching droplets adhesion and transparency via *in situ* electric-actuated reconfigurable shape-memory shutters. *Adv Funct Mater* 2023; **33**: 2210495.

113 Park K, Jin S, Kim G. Transparent window film with embedded nano-shades for thermoregulation. *Constr Build Mater* 2021; **269**: 121280.

114 Li J, Lu X, Zhang Y, *et al.* Transmittance tunable smart window based on magnetically responsive 1D nanochains. *ACS Appl Mater Interfaces* 2020; **12**: 31637–31644.

115 Xie Y, Guan F, Li Z, *et al.* A phase-changing polymer film for broadband smart window applications. *Macromol Rapid Commun* 2020; **41**: 2000290.

116 Li G, Jiang X, Asfahan H, *et al.* Humidity-controlled smart window with synchronous solar and thermal radiation regulation. *Adv Sci* 2025; **12**: e06980.

117 Dai M, Zhao J, Zhang Y, *et al.* Dual-responsive hydrogels with three-stage optical modulation for smart windows. *ACS Appl Mater Interfaces* 2022; **14**: 53314–53322.

118 Fan J, Wakuta T, Hong HJ, *et al.* A transparent semicrystalline polymer used in thermally responsive smart window application. *Adv Funct Mater* 2025; **35**: 2506061.

119 Khandelwal H, Schenning APHJ, Debije MG. Infrared regulating smart window based on organic materials. *Adv Energy Mater* 2017; **7**: 1602209.

120 Barile CJ, Slotcavage DJ, McGehee MD. Polymer-nanoparticle electrochromic materials that selectively modulate visible and near-infrared light. *Chem Mater* 2016; **28**: 1439–1445.

121 Xiao Y, Zhang X, Li Z, *et al.* A visible-to-infrared broadband all-solid-state electrochromic device based $Li_4Ti_5O_{12}$/WO_3 for optical and thermal management. *Sol Energy Mater Sol Cells* 2024; **268**: 112735.

122 Zhou J, Han Y. Design of a widely adjustable electrochromic device based on the reversible metal electrodeposition of Ag nanocylinders. *Nano Res* 2023; **16**: 1421–1429.

123 Uji S, Kimura S, Nakamura K, *et al.* Analysis for coloration mechanism of reversible silver deposition-based electrochromic device by *in situ* observation of plasmonic nanoparticles with dark-field microscopy. *Sol Energy Mater Sol Cells* 2023; **251**: 112119.

124 Li J, Jiang Y, Liu J, *et al.* A photosynthetically active radiative cooling film. *Nat Sustain* 2024; **7**: 786–795.

125 Ionut Bercea A, Champeaux C, Boulle A, *et al.* Adaptive gold/vanadium dioxide periodic arrays for infrared optical modulation. *Appl Surf Sci* 2022; **585**: 152592.

126 Tang Z, Li H, Liu Y, *et al.* Advanced electrochromic properties of Nb-doped WO_3 inverse opal films in NIR region by slow photon effect-assisted enhancement of localized surface plasmon resonance. *Appl Surf Sci* 2023; **622**: 156802.

127 Yu N, Hu Y, Wang X, *et al.* Dynamically tuning near-infrared-induced photothermal performances of TiO_2 nanocrystals by Nb doping for imaging-guided photothermal therapy of tumors. *Nanoscale* 2017; **9**: 9148–9159.

128 Dahlman CJ, Tan Y, Marcus MA, *et al.* Spectroelectrochemical signatures of capacitive charging and ion insertion in doped anatase titania nanocrystals. *J Am Chem Soc* 2015; **137**: 9160–9166.

129 Dou S, Zhao J, Zhang W, *et al.* A universal approach to achieve high luminous transmittance and solar modulating ability simultaneously for vanadium dioxide smart coatings via double-sided localized surface plasmon resonances. *ACS Appl Mater Interfaces* 2020; **12**: 7302–7309.

130 Li K, Zhang Y, Zhang M, *et al.* $AOBiX_2$ (A = La, Tb, Lu; X = S, Se): A family of 2D narrow bandgap semiconductors with high stability, broad-spectrum response, flexibility and high carrier mobility. *J Rare Earths* 2025; doi:10.1016/j.jre.2025.08.010.

131 Tong X, Wang J, Zhang P, *et al.* Insight into the structure-activity relationship in electrochromism of WO_3 with rational internal cavities for broadband tunable smart windows. *Chem Eng J* 2023; **470**: 144130.

132 Jia Y, Liu D, Chen D, *et al.* Transparent dynamic infrared emissivity regulators. *Nat Commun* 2023; **14**: 5087.

133 Tang K, Dong K, Li J, *et al.* Temperature-adaptive radiative coating for all-season household thermal regulation. *Science* 2021; **374**: 1504–1509.

134 Cheng N, Wang Z, Lin Y, *et al.* Breathable dual-mode leather-like nanotextile for efficient daytime radiative cooling and heating. *Adv Mater* 2024; **36**: 2403223.

135 Wang P, Wang H, Sun Y, *et al.* Transparent grating-based metamaterials for dynamic infrared radiative regulation smart windows. *Phys Chem Chem Phys* 2024; **26**: 16253–16260.

136 Jia Y, Liu D, Chen D, *et al.* Realizing sunlight-induced efficiently dynamic infrared emissivity modulation based on aluminum-doped zinc oxide nanocrystals. *Adv Sci* 2024; **11**: 2405962.

137 Jia Y, Liu D, Wang X, *et al.* Dynamically modulating the mid-infrared localized surface plasmon resonance of Al-doped ZnO nanocrystals. *Mater Res Express* 2023; **10**: 095001.

138 Mei Z, Ding Y, Wang M, *et al.* A colorful electrochromic infrared emissivity regulator for all-season intelligent thermal management in buildings. *Adv Mater* 2025; **37**: 2420578.

139 Wang Y, Wang M, Mei Z, *et al.* Intelligent infrared thermal control reflector based on multi-color electrochromic dynamic modulation. *Sol Energy Mater Sol Cells* 2025; **282**: 113362.

140 Li M, Liu D, Cheng H, *et al.* Graphene-based reversible metal electrodeposition for dynamic infrared modulation. *J*

Mater Chem C 2020; **8**: 8538–8545.

141 Tao X, Liu D, Liu T, *et al.* A bistable variable infrared emissivity device based on reversible silver electrodeposition. *Adv Funct Mater* 2022; **32**: 2202661.

142 Zhang M, Wang P, Liu X, *et al.* Responsive metasurface for directional control of laser and thermal emission dynamic regulation. *Adv Mater* 2025; **37**: 2506061.

143 Liu Y, Tian Y, Liu X, *et al.* Intelligent regulation of VO_2-PDMS-driven radiative cooling. *Appl Phys Lett* 2022; **120**: 171704.

144 Huang J, Zhang X, Yu X, *et al.* Scalable self-adaptive radiative cooling film through VO_2-based switchable core-shell particles. *Renew Energy* 2024; **224**: 120208.

145 Cheng B, Cheng H, Jia Y, *et al.* Infrared electrochromic devices based on thin metal films. *Adv Mater Inter* 2023; **10**: 2202505.

146 Cheng B, Liu D, Jia Y, *et al.* Infrared gasochromic devices based on metal thin films. *Adv Opt Mater* 2022; **10**: 2201702.

147 Song Z, Zhang Z, Zhang X, *et al.* Hierarchically structured, Janus optical nanoengineered wastepaper for switchable radiative cooling/heating. *Carbon Energy* 2025; **7**: e676.

148 Yang P, He J, Ju Y, *et al.* Dual-mode integrated Janus films with highly efficient NaH_2PO_2-enhanced infrared radiative cooling and solar heating for year-round thermal management. *Adv Sci* 2023; **10**: 2206176.

149 Zhang X, Zhang T, Cao Y, *et al.* A Janus infrared emission dual-mode super-fabric for sustainable efficient thermal management. *Chem Eng J* 2025; **503**: 158664.

150 Du Z, Li M, Xu S, *et al.* VO_2-based intelligent thermal control coating for spacecraft by regulating infrared emittance. *J Alloys Compd* 2022; **895**: 162679.

151 Fan C, Zhang Y, Long Z, *et al.* Dynamically tunable subambient daytime radiative cooling metafabric with janus wettability. *Adv Funct Mater* 2023; **33**: 2300794.

152 Pian S, Wang Z, Lu C, *et al.* Scalable colored Janus fabric scheme for dynamic thermal management. *iScience* 2024; **27**: 110948.

153 Wei L, Lin G, Liu J, *et al.* Conductive structural colored cotton fabrics with nonangle-dependent colors and dynamic thermal management. *ACS Appl Mater Interfaces* 2025; **17**: 21985–21995.

154 Chow L, Zhang Q, Huang X, *et al.* Army ant nest inspired adaptive textile for smart thermal regulation and healthcare monitoring. *Adv Mater* 2025; **37**: 2406798.

155 Li GX, Dong T, Zhu L, *et al.* Microfluidic-blow-spinning fabricated sandwiched structural fabrics for all-season personal thermal management. *Chem Eng J* 2023; **453**: 139763.

156 Xue T, Chen X, Wang C, *et al.* Dual-mode cellulose acetate@Al_2O_3/MWCNTs Janus fabric with radiative cooling and solar heating for personal thermal management. *Chem Eng J* 2024; **500**: 156713.

157 Ma R, Xue T, Han T, *et al.* Dual mode switchable Janus Nano-ZnO/rGO cellulose fabric with radiative regulation and sweat transport for personal thermal management. *Chem Eng J* 2025; **520**: 165707.

158 Ding C, Lin Y, Cheng N, *et al.* Dual-cooling textile enables vertical heat dissipation and sweat evaporation for thermal and moisture regulation. *Adv Funct Mater* 2024; **34**: 2400987.

159 Zhang Y, Fu J, Ding Y, *et al.* Thermal and moisture managing e-textiles enabled by Janus hierarchical gradient honeycombs. *Adv Mater* 2024; **36**: 2311633.

160 Xiao Y, Chen Z, Zheng W, *et al.* A Janus fabric composed of temperature-adaptive phase-changing and radiative cooling layers for dynamic personal thermal management. *Chem Eng J* 2025; **521**: 166795.

161 Zhao Z, Li H, Peng Y, *et al.* Hierarchically programmed meta-louver fabric for adaptive personal thermal management. *Adv Funct Mater* 2024; **34**: 2404721.

162 Lan C, Liang M, Meng J, *et al.* Humidity-responsive actuator-based smart personal thermal management fabrics achieved by solar thermal heating and sweat-evaporation cooling. *ACS Nano* 2025; **19**: 8294–8302.

163 Fan Q, Fan H, Han H, *et al.* Dynamic thermoregulatory textiles woven from scalable-manufactured radiative

electrochromic fibers. *Adv Funct Mater* 2024; **34**: 2310858.

164 Zhu J, Zhu P, Sun H, *et al.* Dynamically adaptive wrinkle-structured light-regulating films for energy-efficient buildings. *Adv Funct Mater* 2025; e10262.

165 Zhang X, Li H, Xie N, *et al.* Laboratorial investigation on optical and thermal properties of thermochromic pavement coatings for dynamic thermoregulation and urban heat island mitigation. *Sustain Cities Soc* 2022; **83**: 103950.

166 Park C, Lee W, Park C, *et al.* Efficient thermal management and all-season energy harvesting using adaptive radiative cooling and a thermoelectric power generator. *J Energy Chem* 2023; **84**: 496–501.

167 Liu B, Wu J, Xue C, *et al.* Bioinspired superhydrophobic all-in-one coating for adaptive thermoregulation. *Adv Mater* 2024; **36**: 2400745.

168 Yuan H, Liu R, Cheng S, *et al.* Scalable fabrication of dual-function fabric for zero-energy thermal environmental management through multiband, synergistic, and asymmetric optical modulations. *Adv Mater* 2023; **35**: 2209897.

169 Feng S, Yao L, Feng M, *et al.* Regeneration of pea-pod-like cellulose acetate fibers as aerogel-derived boards for building thermal regulation and carbon reduction. *Adv Fiber Mater* 2024; **6**: 570–582.

170 Zeng S, Shen K, Liu Y, *et al.* Dynamic thermal radiation modulators via mechanically tunable surface emissivity. *Mater Today* 2021; **45**: 44–53.

171 Wang P, Xie W, Zhang J, *et al.* Dual-functional photonic battery enabling dynamic radiative thermal management and power supply. *Adv Mater* 2025; **37**: 2412328.

172 Song X, Gong H, Li H, *et al.* Molecularly and structurally designed polyimide nanofiber radiative cooling films for spacecraft thermal management. *Adv Funct Mater* 2025; **35**: 2413191.

173 Dong K, Tseng D, Li J, *et al.* Reducing temperature swing of space objects with temperature-adaptive solar or radiative coating. *Cell Rep Phys Sci* 2022; **3**: 101066.

174 Yang J, Li Q, Liu S, *et al.* Temperature-adaptive metasurface radiative cooling device with excellent emittance and low solar absorptance for dynamic thermal regulation. *Adv Photon* 2024; **6**: 046006.

175 Xie B, Dong J, Zhao J, *et al.* VO_2 particle-based intelligent metasurface with perfect infrared emission for the spacecraft thermal control. *Appl Opt* 2022; **61**: 10538.

176 Chen Q, Li C, Huang X, *et al.* Ultrabroadband directional tunable thermal emission control based on vanadium dioxide photonic structures. *Adv Sci* 2025; **12**: 2416437.

177 Wu B, Huang X, Wu X. Transparent smart radiation device for efficient thermal management of spacecraft solar cells. *Case Studies Therm Eng* 2025; **71**: 106161.

178 Singh L, Qiu E, Cardin AE, *et al.* Passive radiative thermal management using phase-change metasurfaces. *J Phys Photonics* 2025; **7**: 025028.

179 Xu D, Zhao J, Liu L. Near-field radiation assisted smart skin for spacecraft thermal control. *Int J Therm Sci* 2021; **165**: 106934.

180 Lee SJ, Choi SY, Song SY. Experimental evaluation study of the comfort and energy performance of suspended particle device smart windows in a residential building: Achieving optimal control during the cooling season. *J Build Eng* 2024; **98**: 111176.

181 Li Z, Zhao S, Shao Z, *et al.* Deterioration mechanism of vanadium dioxide smart coatings during natural aging: Uncovering the role of water. *Chem Eng J* 2022; **447**: 137556.

182 Li Z, Cao C, Li M, *et al.* Gradient variation oxygen-content vanadium-oxygen composite films with enhanced crystallinity and excellent durability for smart windows. *ACS Appl Mater Interfaces* 2023; **15**: 9401–9411.

183 Beebe MR, Klopf JM, Wang Y, *et al.* Time-resolved light-induced insulator-metal transition in niobium dioxide and vanadium dioxide thin films. *Opt Mater Express* 2017; **7**: 213.

184 Robinson ZR, Beckmann K, Michels J, *et al.* Measurement of the crystallization and phase transition of niobium dioxide thin-films using a tube furnace optical transmission system. *AIP Adv* 2024; **14**: 115113.

185 Ji H, Liu D, Cheng H, *et al.* Inkjet printing of vanadium dioxide nanoparticles for smart windows. *J Mater Chem C* 2018; **6**: 2424–2429.

186 Wang N, Duchamp M, Dunin-Borkowski RE, *et al.* Terbium-doped VO_2 thin films: Reduced phase transition temperature and largely enhanced luminous transmittance. *Langmuir* 2016; **32**: 759–764.

187 Zhang L, Sun H, Liu H, *et al.* The investigation of wrinkled ZnO as antireflective, protective, hydrophobic layer on the thermochromic VO_2 films for smart windows. *Appl Phys A* 2025; **131**: 222.

188 Jung KH, Yun SJ, Slusar T, *et al.* Highly transparent ultrathin vanadium dioxide films with temperature-dependent infrared reflectance for smart windows. *Appl Surf Sci* 2022; **589**: 152962.

189 Inomata N, Usuda T, Yamamoto Y, *et al.* Effects of temperature and doping concentration on the piezoresistive property of vanadium dioxide thin film. *Sens Actuat A-Phys* 2022; **346**: 113823.

190 Ko B, Chae JY, Badloe T, *et al.* Multilevel absorbers via the integration of undoped and tungsten-doped multilayered vanadium dioxide thin films. *ACS Appl Mater Interfaces* 2022; **14**: 1404–1412.

191 White ST, Taylor JR, Chukhryaev I, *et al.* Solid-state dewetting of tungsten-doped vanadium dioxide nanoparticles: Implications for thermochromic coatings. *ACS Appl Nano Mater* 2025; **8**: 9972–9980.

192 Suzuki N, Xue Y, Hasegawa T, *et al.* Phase transition behavior and optical properties of F/Mo co-doped VO_2 for smart windows. *Sol Energy Mater Sol Cells* 2023; **251**: 112105.

193 Geng X, Chang T, Fan J, *et al.* Tuning phase transition and thermochromic properties of vanadium dioxide thin films via cobalt doping. *ACS Appl Mater Interfaces* 2022; **14**: 19736–19746.

194 Koch D, Chaker M. The origin of the thermochromic property changes in doped vanadium dioxide. *ACS Appl Mater Interfaces* 2022; **14**: 23928–23943.

195 Zhao S, Tao Y, Chen Y, *et al.* Room-temperature synthesis of inorganic-organic hybrid coated VO_2 nanoparticles for enhanced durability and flexible temperature-responsive near-infrared modulator application. *ACS Appl Mater Interfaces* 2019; **11**: 10254–10261.

196 Chang T, Cao X, Li N, *et al.* Facile and low-temperature fabrication of thermochromic Cr_2O_3/VO_2 smart coatings: Enhanced solar modulation ability, high luminous transmittance and UV-shielding function. *ACS Appl Mater Interfaces* 2017; **9**: 26029–26037.

197 Chang T, Cao X, Li N, *et al.* Mitigating deterioration of vanadium dioxide thermochromic films by interfacial encapsulation. *Matter* 2019; **1**: 734–744.

198 Wang L, Li Z, Cao C, *et al.* Facile and dynamic infrared modulation of durable VO_2/CuI films for smart window applications. *Chem Eng J* 2024; **488**: 150972.

199 Li H, Zhang X, Zhu M, *et al.* All-solid-state transparent-to-black electrochromic smart window for building energy saving. *ACS Energy Lett* 2025; **10**: 4148–4157.

200 Zhu M, Cao S, Wang S, *et al.* Unveiling the electrochromic switch: The π spacer's pivotal role in fluorinated D-A copolymer for high color efficiency and energy-saving smart windows. *Nano Energy* 2025; **142**: 111240.

201 Jia Z, Sui Y, Qian L, *et al.* Electrochromic windows with fast response and wide dynamic range for visible-light modulation without traditional electrodes. *Nat Commun* 2024; **15**: 6110.

202 Ning W, Zhao X, Klarbring J, *et al.* Thermochromic lead-free halide double perovskites. *Adv Funct Mater* 2019; **29**: 1807375.

203 Rosales BA, Kim J, Wheeler VM, *et al.* Thermochromic halide perovskite windows with ideal transition temperatures. *Adv Energy Mater* 2023; **13**: 2203331.

204 Kamal W, Li M, Lin J, *et al.* Spatially patterned polymer dispersed liquid crystals for image-integrated smart windows. *Adv Opt Mater* 2022; **10**: 2101748.

205 Pathinti RS, Tatipamula AK, Vallamkondu J. ZnO nanoparticles dispersed cholesteric liquid crystal based smart window for energy saving application. *J Alloys Compd* 2023; **963**: 171198.

206 Tu H, Wang T, Chen M, *et al.* Isotope-driven hydrogel smart windows for self-adaptive thermoregulation. *Nat Commun* 2025; **16**: 6952.

207 Li X, Cao C, Liu C, *et al.* Self-rolling of vanadium dioxide nanomembranes for enhanced multi-level solar modulation. *Nat Commun* 2022; **13**: 7819.

208 Li G, Chen J, Yan Z, *et al.* Physical crosslinked hydrogel-derived smart windows: Anti-freezing and fast thermal responsive performance. *Mater Horiz* 2023; **10**: 2004–2012.

209 Zhu G, Gang Xu G, Zhang Y, *et al.* Thermochromic smart windows with ultra-high solar modulation and ultra-fast responsive speed based on solid-liquid switchable hydrogels. *Research* 2024; **7**: 0462.

210 Xing C, Yang L, He R, *et al.* Brookite TiO_2 nanorods as promising electrochromic and energy storage materials for smart windows. *Small* 2023; **19**: 2303639.

211 Shao Z, Huang A, Ming C, *et al.* All-solid-state proton-based tandem structures for fast-switching electrochromic devices. *Nat Electron* 2022; **5**: 45–52.

212 Sun J, Chen Z, Zhang R, *et al.* Electrochromic smart windows with co-intercalation of cations and anions for multi-band regulations. *Nat Commun* 2025; **16**: 6993.

213 Sheng SZ, Wang JL, Zhao B, *et al.* Nanowire-based smart windows combining electro- and thermochromics for dynamic regulation of solar radiation. *Nat Commun* 2023; **14**: 3231.

214 Tao J, Tian S, Li B, *et al.* Photo-thermochromic $W_{18}O_{49}$/hydrogel hybrid smart windows for graded and dual-band sunlight control. *Chem Eng J* 2024; **482**: 149079.

215 Zhang Y, Ding Y, Lan F, *et al.* A photo- and electrochromic dual-responsive smart window for full-day photothermal management. *Small* 2025; **21**: 2501977.

216 Cao S, Zhang S, Zhang T, *et al.* A visible light-near-infrared dual-band smart window with internal energy storage. *Joule* 2019; **3**: 1152–1162.

217 Liu R, Li Y, Hu B, *et al.* Organic ligand-free scalable dual-band electrochromic smart windows. *Adv Funct Mater* 2025; **35**: 2409914.

218 Zhou Y, Lv Y, Guo X, *et al.* Electrochromic smart windows with on-demand photothermal regulation for energy-saving buildings. *Adv Mater* 2025; **37**: 2502706.

219 Wang S, Jiang T, Meng Y, *et al.* Scalable thermochromic smart windows with passive radiative cooling regulation. *Science* 2021; **374**: 1501–1504.

220 Zhang Z, Yu M, Ma C, *et al.* A Janus smart window for temperature-adaptive radiative cooling and adjustable solar transmittance. *Nano-Micro Lett* 2025; **17**: 233.

221 Zhang H, Zhang X, Sun W, *et al.* All-solid-state transparent variable infrared emissivity devices for multi-mode smart windows. *Adv Funct Mater* 2024; **34**: 2307356.

222 Shao Z, Huang A, Cao C, *et al.* Tri-band electrochromic smart window for energy savings in buildings. *Nat Sustain* 2024; **7**: 796–803.